COMMUN. MATH. SCI.
Vol. 19, No. 1, pp. 147–174

NORMALIZED GOLDSTEIN-TYPE LOCAL MINIMAX METHOD FOR FINDING MULTIPLE UNSTABLE SOLUTIONS OF SEMILINEAR ELLIPTIC PDES*

WEI LIU†, ZIQING XIE‡, AND WENFAN YI§

Abstract. In this paper, we propose a normalized Goldstein-type local minimax method (NG-LMM) to seek for multiple minimax-type solutions. Inspired by the classical Goldstein line search rule in the optimization theory in $\mathbb{R}^m$, which is aimed to guarantee the global convergence of some descent algorithms, we introduce a normalized Goldstein-type search rule and combine it with the local minimax method to be suitable for finding multiple unstable solutions of semilinear elliptic PDEs both in numerical implementation and theoretical analysis. Compared with the normalized Armijo-type local minimax method (NA-LMM), which was first introduced in [Y. Li and J. Zhou, SIAM J. Sci. Comput., 24(3):865–885, 2002] and then modified in [Z.Q. Xie, Y.J. Yuan, and J. Zhou, SIAM J. Sci. Comput., 34(1):A395–A420, 2012], our approach can prevent the step-size from being too small automatically and then ensure that the iterations make reasonable progress by taking full advantage of two inequalities. The feasibility of the NG-LMM is verified strictly. Further, the global convergence of the NG-LMM is proven rigorously under a weak assumption that the peak selection is only continuous. Finally, it is implemented to solve several typical semilinear elliptic boundary value problems on square or dumbbell domains for multiple unstable solutions and the numerical results indicate that this approach performs well.

Keywords. semilinear elliptic PDEs; global convergence; multiple solutions; local minimax method; normalized Goldstein-type search rule.

AMS subject classifications. 35J20; 35B38; 65K15; 65N12.

1. Introduction

Consider to find multiple solutions to the Euler-Lagrange equation

$$J'(u)=0, \tag{1.1}$$

where J, called a generic energy functional, is a C^1-functional on a Hilbert space H, and J' is its Fréchet derivative. The solutions to the Euler-Lagrange Equation (1.1) are corresponding to the critical points of J. The most well-known critical points are the local minima (maxima), which the classical variational or optimization theories focus on. In contrast, a critical point, which is not a local extremum, is called a saddle point. Actually a saddle point u^* of J is a critical point, whose any neighborhood in H contains points v and w such that $J(v)<J(u^*)<J(w)$. Saddle points are unstable and will be the main concern in this paper.

From Morse theory, for a critical point u^*, let $H=H^-\oplus H^0\oplus H^+$, where H^-, H^0 and H^+ are, respectively, the maximum negative definite, null and maximum positive definite orthogonal subspaces of the linear operator $J''(u^*)$ in H with $\dim(H^0)<\infty$. Then the Morse index (MI) of u^* is defined as the dimension of H^-, i.e., $\mathrm{MI}(u^*)=\dim(H^-)$. For instance, a local minimum of the energy functional J is a solution of

*Received: December 16, 2019; Accepted (in revised form): August 12, 2020. Communicated by Shi Jin.

†Key Laboratory of Computing and Stochastic Mathematics (LCSM)(Ministry of Education), School of Mathematics and Statistics, Hunan Normal University, Changsha 410081, P.R. China (wliu.hunnu@foxmail.com).

‡Corresponding author. LCSM (MOE), School of Mathematics and Statistics, Hunan Normal University, Changsha 410081, P.R. China (ziqingxie@hunnu.edu.cn).

§Institute of Mathematics, School of Mathematics, Hunan University, Changsha 410082, P.R. China (wfyi@hnu.edu.cn).

(1.1) with MI $=0$. As a matter of fact, the Morse index is an important concept that provides information of the local structure of a critical point and is used to describe its instability. Actually the higher the Morse index is, the more unstable the critical point is.

Multiple saddle points with different performance and instability indices exist in many nonlinear problems in the natural and social sciences [2,4,12,20,21,26,30–32]. In physics, chemistry and materials sciences, saddle points appear as unstable equilibria or transient excited states of the energy surface. They are usually used to study the rare transition of different stable states or metastable states, and play a significant role in determining the physical and chemical properties of substances such as nucleation and reaction rate. Due to the difficulties and challenges in making direct experimental observation, several computational methods have been developed for computing saddle points, e.g., string method, gentlest ascent method and dimer method, etc., for which we refer to [6,8–10,13,29] and references therein. It is noted that the numerical methods above are mainly aimed to find the saddle points with MI $=1$. With the development of science and technology, nowadays more and more attention is paid to both theory and application to solve numerically for multiple unstable critical points with higher Morse index in a stable way.

Inspired by the numerical work of Choi-McKenna [5], Ding-Costa-Chen [7] and Chen-Zhou-Ni [3], a local minimax method (LMM) that characterizes a saddle point as a solution to a local minimax problem was established in Li-Zhou's work [15]. Based on the local characterization, a numerical local minimax algorithm was designed for finding multiple saddle points [15,16]. Roughly speaking, the LMM characterizes a saddle point of J as a solution to the following two-level local optimization problem [15, 16, 26, 28]: Find $u^* \in H$ s.t.

$$J(u^*) = \min_{v \in S_H} \max_{u \in [L,v]} J(u), \tag{1.2}$$

where $S_H = \{v \in H : \|v\| = 1\}$ is the unit sphere with $\|\cdot\|$ the norm in H, $L \subset H$ is a given finite-dimensional closed subspace and $[L,v] = \{tv + w : w \in L, t \geq 0\}$. It is apparent that the local maximization in the first level is actually an optimization problem in the finite-dimensional half subspace $[L,v]$. Consequently some standard numerical optimization algorithms can be conveniently implemented to solve it. Nevertheless, the local minimization in the second level is more challenging as it works in the unit sphere S_H, which is infinite-dimensional. In the LMM, the steepest descent direction serves as the search direction in the local minimization process. As a matter of fact, this strategy has been widely applied for solving various multiple solution problems. For this topic, we refer to [26–28, 33] and references therein.

On the other hand, to guarantee the robustness of the numerical methods, the large-scope or even global convergence is always one of the main issues to the descent algorithms for solving optimization problems or nonlinear equations. It is known that the line search rule is one of the efficient strategies to find a suitable step-size and guarantee the global convergence of the numerical methods to the optimization problems [14, 22, 23]. In the optimization theory, for a given objective function f defined in $\mathbb{R}^m$, the aim of the line search is to find a step-size $s^k > 0$ along a descent direction d^k starting from x^k, s.t.,

$$f(x^k + s^k d^k) < f(x^k). \tag{1.3}$$

If the step-size s^k is determined by minimizing the objective function along the descent direction d^k starting from x^k, i.e.,

$$f(x^k+s^kd^k)=\min_{s>0} f(x^k+sd^k), \tag{1.4}$$

it is called an exact line search rule with s^k the optimal step-size. Though there exist several exact line search algorithms in the literature, they are not popular since they are often expensive. In contrast, if the step-size s^k is chosen such that the descent amount $f(x^k)-f(x^k+s^kd^k)>0$ is acceptable, this line search rule is called an inexact one. Due to their efficiency and much cheaper computational cost compared with the exact line search strategies, the inexact line search rules are highly preferred in practice. In the literature the well-known inexact line search rules include the Armijo rule [1], Goldstein rule [11] and Wolfe-Powell rule [19, 24, 25], etc..

As mentioned above, the LMM is aimed to find the local optimal solution $u^*\in H$ for the two-level optimization problem (1.2). Once v^k and u^k are obtained, the LMM tries to find

$$v^{k+1}=v^k(s^k)=\frac{v^k+s^kd^k}{\|v^k+s^kd^k\|}, \quad u^{k+1}=p(v^k(s^k)), \tag{1.5}$$

by some search rules, where $s^k>0$ is a step-size, $d^k\in H$ is the steepest descent direction of J at u^k, and $p(v^k(s^k))$ represents a local maximizer of J on the finite-dimensional half subspace $[L,v^k(s^k)]$ and can be expressed as $p(v^k(s^k))=t^kv^k(s^k)+w_L^k\in[L,v^k(s^k)]$ for some $t^k\geq 0$ and $w_L^k\in L$. Actually $p(v^k(s^k))$ denotes a local peak selection of J w.r.t. L at $v^k(s^k)$, an important concept which will be introduced in Section 2. Since the sequence $\{v^k\}\subset S_H$ generated by the algorithm of the LMM is constrained on a unit sphere, the line search strategies in the optimization theory have to be updated so that they are suitable for this new situation. Actually in [15], the idea of line search in the optimization theory in $\mathbb{R}^m$ was borrowed for the first time with a normalized modification to adapt for the generic nonlinear functional with a minimax structure. They tried to find $s^k>0$ such that $J(p(v^k(s)))$ at s^k is minimized, i.e.,

$$J(p(v^k(s^k)))=\min_{s>0} J(p(v^k(s))), \tag{1.6}$$

with s^k the optimal step-size [15]. However, such a step-size rule is a kind of exact one and is not convenient for both numerical implementation and convergence analysis. Moreover, it is even more expensive and complicated than its partner in the optimization theory. In fact, $J(p(v))$ is a composite functional of J, p and v, and the update $v^{k+1}=v^k(s^k)$ is nonlinear in terms of s^k, while the update $x^{k+1}=x^k(s^k)=x^k+s^kd^k$ is linear w.r.t. s^k in the optimization theory.

As a result, we concentrate on some inexact step-size search rules in the following, i.e., the step-size s^k is chosen such that the descent amount $J(p(v^k))-J(p(v^k(s^k)))>0$ is acceptable by tolerance. In the literature, the normalized Armijo-type search rule was first introduced in [16] and further developed as the following simpler form in [28], i.e.,

$$J(p(v^k(s^k)))-J(p(v^k))\leq -\frac{1}{4}t^ks^k\|d^k\|^2, \tag{1.7}$$

where the factor $\frac{1}{4}$ can be substituted by any constant σ with $0<\sigma<1$. Once s^k satisfies the condition (1.7), $u^{k+1}=p(v^k(s^k))$ is a new acceptable approximation. Here, the step-size s^k is determined by a backtracking strategy [16, 23]. This algorithm is much easier to be implemented practically than the former version. Meanwhile, thanks to this update, the convergence of the algorithm was established in [16]. Then the LMM was further modified in [26] by a significant relaxation for the domain of the local peak selection. The global convergence analysis for this modified version was also provided by overcoming the lack of homeomorphism of the local peak selection due to the relaxation for the domain of the local peak selection. Moreover, since the decrease condition (1.7) is satisfied for all sufficiently small $s^k > 0$, the normalized Armijo-type search rule combined with a backtracking strategy is always feasible. Nevertheless, a choice of an appropriate backtracking factor is not known a priori. Therefore some safeguards are needed in order to prevent s^k from being too small and not terminating. For example, with an appropriately small least step $s_{\min} > 0$ given, if (1.7) is not satisfied but $s^k\|d^k\| < s_{\min}$, the search has to stop artificially.

The purpose of our effort is to combine new search rules with the LMM for finding multiple unstable solutions of semilinear PDEs. It is noted that, to overcome the drawback of the artificial control of the step-size in the classical Armijo line search rule in the optimization theory, the Goldstein line search rule is introduced [14, 22, 23]. Actually it is composed of two conditions: one guarantees the decrease, and the other enables the step-size not to be too small. As a result, it turns to be one of the most popular line search rules. Inspired by the success of the normalized Armijo-type local minimax method (NA-LMM) and the Goldstein line search rule in the optimization theory, this paper is aimed to establish the normalized Goldstein-type local minimax method (NG-LMM) for finding multiple minimax-type solutions of the Euler-Lagrange Equation (1.1), and provide its mathematical justification and global convergence analysis.

This paper is organized as follows. In Section 2, we give some preliminaries for our work. Secondly, the normalized Goldstein search rule is given and its feasibility and some related properties are provided in Section 3 and then, Section 4 presents the normalized Goldstein-type local minimax algorithm (NG-LMA) in details. In Section 5 the global convergence of NG-LMA is verified strictly. Further, Section 6 is devoted to exhibit some numerical results by implementing our approach for finding multiple unstable solutions of Lane-Emden equation, Henon equation and the limiting stationary Gierer-Meinhardt equation on square or dumbbell domains. All these numerical results and analysis illustrate the effectiveness and robustness of the approach. Finally, some concluding remarks are given in Section 7.

2. Preliminaries

In order to depict our method, it is necessary to introduce some notations and background as preliminaries.

Let $\|\cdot\|$ be the norm induced by the inner product $\langle\cdot,\cdot\rangle_H$ of the Hilbert space H. For some finite-dimensional closed subspace $L \subset H$, its orthogonal complement is denoted by $L^\perp$. Then each $v \in H$ can be decomposed into $v = v_L + v_\perp$, where $v_L \in L$ and $v_\perp \in L^\perp$. It is worthy to point out that the subspace L can be flexibly determined in practice. Actually, in our numerical algorithm it is simply taken as the span of some previously found critical points. This choice of L can guarantee that the computed solution is different from those in L (see the details in Sections 4 or 6) and thus a new one.

Denote $S_H = \{v \in H : \|v\| = 1\}$ as the unit sphere in H. For each $v \in S_H$, we define a closed half-subspace $[L, v] = \{tv + w : w \in L, t \geq 0\}$. The local peak selection is defined as follows.

Definition 2.1 (Local peak selection [26]). *Denote 2^H as the set of all subsets of H.*

The set-valued peak mapping $P: S_H \to 2^H$ w.r.t. L is defined by

$$P(v) := \{u^* | J(u^*) = \max_{u \in [L,v]} J(u)\}, \quad \forall v \in S_H.$$

A single-valued mapping $p: S_H \to H$ is called a peak selection of J w.r.t. L if

$$p(v) \in P(v), \quad \forall v \in S_H.$$

For a given $v \in S_H$, we say that J has a local peak selection w.r.t. L at v if there is a neighborhood $\mathcal{N}(v)$ of v and a mapping $p: \mathcal{N}(v) \cap S_H \to H$ such that

$$p(u) \in P(u), \quad \forall u \in \mathcal{N}(v) \cap S_H.$$

With the definition of the local peak selection p of J w.r.t. L in hands, a solution submanifold is defined as

$$\mathcal{M} = \big\{p(v) \,\big|\, p(v) \in P(v), v \in S_H\big\}. \tag{2.1}$$

The idea of the solution submanifold (2.1) is dated from [17], in which Nehari introduced it to study a dynamical system. Then in [18], Ding-Ni used Nehari's idea to investigate a semilinear elliptic problem with homogeneous Dirichlet boundary condition. They introduced a solution submanifold which is actually a special case of $\mathcal{M}$ defined in (2.1) when $L = \{0\}$.

According to [26], the target of the LMM is to find the local minimizer u^* of J on the submanifold $\mathcal{M}$, i.e.,

$$J(u^*) = \min_{u \in \mathcal{M}} J(u). \tag{2.2}$$

By the definition, the local peak selection $p(v)$ is a local maximum point of J on the half subspace $[L,v]$. Thus (2.2) is equivalent to the two-level local optimization problem of the form (1.2). In addition, if a saddle point of J, which is an unstable critical point in H, is characterized by (2.2), then it becomes stable on the submanifold $\mathcal{M}$. Then, some descent search algorithms can be implemented to deal with this problem. In the LMM, the steepest descent direction serves as the search direction in the local minimization process (2.2). However, it has to be mentioned that, the smoothness of $J'(w) \in H^*$, with H^* the duality of H (e.g., $H^* = H^{-1}(\Omega)$ for $H = H^1(\Omega)$), is usually "poor" and cannot serve as a search direction in H. Instead, the Riesz representer of $-J'(u)$ in H, denoted by $d = -\nabla J(u) \in H$, is used as an appropriate search direction and also called the steepest descent direction, which is determined by

$$\langle d, \phi \rangle_H = -\langle J'(u), \phi \rangle, \quad \forall \phi \in H, \tag{2.3}$$

with $\langle \cdot, \cdot \rangle$ the duality pairing between H and its dual space H^*. It will be seen that, in numerical implementation, d can be obtained by several classical numerical methods, e.g., the finite element method, and so on.

3. Normalized Goldstein search rule and its feasibility

The classical Goldstein line search rule [11, 23] in the optimization theory in the Euclidean space for a given objective function f is usually expressed as

$$\sigma_1 s^k \nabla f(x^k)^T d^k \le f(x^k + s^k d^k) - f(x^k) \le \sigma_2 s^k \nabla f(x^k)^T d^k,$$

with d^k a descent direction of $f(x)$ at x^k, for some constants σ_1 and σ_2 satisfying $0<\sigma_2<\sigma_1<1$. Motivated by it, we introduce a normalized Goldstein search rule for finding multiple saddle-point solutions of semilinear PDEs in this section.

For simplicity, set $H=H_0^1(\Omega)$ or $H^1(\Omega)$, unless specified. Denote $v=v_L+v_\perp\in S_H$ and $p(v)=tv+w_L\in[L,v]$, with $p(v)$ the local peak selection of J w.r.t. L at v, where $v_L,w_L\in L$, $v_\perp\in L^\perp$ and $v_\perp\neq 0$. Let $d=-\nabla J(p(v))$ defined in (2.3). The definition of the local peak selection $p(v)$ and the relation between $-J'(p(v))$ and d imply the following orthogonality properties.

Lemma 3.1 ([26]).
(i) $J'(p(v))\perp[L,v]$ *and* $J'(p(v))\perp p(v)$ *w.r.t. the duality pairing* $\langle\cdot,\cdot\rangle$*;*
(ii) $d\perp[L,v]$ *and* $d\perp p(v)$ *w.r.t. the inner product* $\langle\cdot,\cdot\rangle_H$*.*

It is observed that

$$v(s)=\frac{v+sd}{\|v+sd\|}=\frac{v_L}{\sqrt{1+s^2\|d\|^2}}+\frac{v_\perp+sd}{\sqrt{1+s^2\|d\|^2}}:=v_L(s)+v_\perp(s), \tag{3.1}$$

with

$$v_L(s)=\frac{v_L}{\sqrt{1+s^2\|d\|^2}},\qquad v_\perp(s)=\frac{v_\perp+sd}{\sqrt{1+s^2\|d\|^2}}. \tag{3.2}$$

By Lemma 3.1, it holds that $v_L(s)\in L$ and $v_\perp(s)\in L^\perp$. In addition, we have the following property for $v_\perp(s)$.

Lemma 3.2. *For $v(s)$ expressed as in* (3.1)*, it holds that* $\|v_\perp(s)\|\geq\|v_\perp\|>0$.

Proof. A direct calculation shows that

$$\|v_\perp(s)\|^2=\|v(s)\|^2-\|v_L(s)\|^2=1-\frac{\|v_L\|^2}{1+s^2\|d\|^2}\geq 1-\|v_L\|^2=\|v_\perp\|^2>0.$$

The conclusion is obtained. ∎

Denote the local peak selection of J w.r.t. L at $v(s)$ as $p(v(s))=t_sv(s)+w_{L,s}\in[L,v(s)]$, where $w_{L,s}\in L$. The normalized Goldstein search rule is introduced as follows.

Definition 3.1 (The normalized Goldstein search rule). *Let $p(v)=tv+w_L$, with $t>0$ and $w_L\in L$, be the local peak selection of J w.r.t. L at v. For two constants σ_1 and σ_2 with $0<\sigma_2<\sigma_1<1$, if $s>0$ satisfies*

$$-\sigma_1ts\|d\|^2<J(p(v(s)))-J(p(v))<-\sigma_2ts\|d\|^2, \tag{3.3}$$

then it is said that the step-size s satisfies the normalized Goldstein search rule w.r.t. L at v.

Before we prove the feasibility of the normalized Goldstein search rule, we should discuss some related properties in the following.

Lemma 3.3. *For any point $v\in S_H$ satisfying $d=-\nabla J(p(v))\neq 0$, it holds that*

$$\frac{s\|d\|}{\sqrt{1+s^2\|d\|^2}}<\|v(s)-v\|<s\|d\|,\quad\forall s>0. \tag{3.4}$$

Furthermore,

$$\lim_{s\to 0^+}\frac{\|v(s)-v\|}{s\|d\|}=1. \tag{3.5}$$

Proof. A straightforward calculation leads to

$$\begin{aligned}\|v(s)-v\| &= \left\|\frac{v+sd}{\|v+sd\|}-v\right\| \\ &= \frac{1}{\sqrt{1+s^2\|d\|^2}}\left\|(1-\sqrt{1+s^2\|d\|^2})v+sd\right\| \\ &= \frac{1}{\sqrt{1+s^2\|d\|^2}}\left\|\frac{-s^2\|d\|^2}{1+\sqrt{1+s^2\|d\|^2}}v+sd\right\| \\ &= \frac{s\|d\|}{\sqrt{1+s^2\|d\|^2}}\sqrt{1+\frac{s^2\|d\|^2}{(1+\sqrt{1+s^2\|d\|^2})^2}},\end{aligned} \tag{3.6}$$

in which the fact $d\perp v$ is used. Thus

$$\frac{s\|d\|}{\sqrt{1+s^2\|d\|^2}} < \|v(s)-v\| < s\|d\|, \quad \forall s>0. \tag{3.7}$$

It further implies that

$$\lim_{s\to 0^+}\frac{\|v(s)-v\|}{s\|d\|}=1. \tag{3.8}$$

□

LEMMA 3.4. *Let $\bar{v}\in S_H$ with $\bar{v}_\perp\neq 0$. Suppose that the local peak selection p w.r.t. L is continuous at $\bar{v}$. Set $p(v)=t_v v+w_L$ and $p(\bar{v})=t_{\bar{v}}\bar{v}+\bar{w}_L$. If $v\to\bar{v}$, then $t_v\to t_{\bar{v}}$ and $w_L\to\bar{w}_L$.*

Proof. Due to the decomposition of $v=v_\perp+v_L$ and $\bar{v}=\bar{v}_\perp+\bar{v}_L$, $v\to\bar{v}$ implies $v_\perp\to\bar{v}_\perp\neq 0$ immediately. On the other hand, by the continuity of p at $\bar{v}$, when $v\to\bar{v}$,

$$\|p(v)-p(\bar{v})\|^2=\|t_v v_\perp - t_{\bar{v}}\bar{v}_\perp\|^2+\|t_v v_L - t_{\bar{v}}\bar{v}_L + w_L-\bar{w}_L\|^2\to 0.$$

As a result, $\|t_v v_\perp - t_{\bar{v}}\bar{v}_\perp\|\to 0$. Therefore

$$t_v=\frac{\|t_v v_\perp\|}{\|v_\perp\|}\to\frac{\|t_{\bar{v}}\bar{v}_\perp\|}{\|\bar{v}_\perp\|}=t_{\bar{v}}, \tag{3.9}$$

where the fact that $\|\bar{v}_\perp\|\neq 0$ is employed. Furthermore, we have

$$w_L=p(v)-t_v v\to p(\bar{v})-t_{\bar{v}}\bar{v}=\bar{w}_L.$$

□

Furthermore, Lemma 3.3 and Lemma 3.4 imply the following lemma directly.

LEMMA 3.5. *Denote $p(v)=tv+w_L$ and $p(v(s))=t_s v(s)+w_{L,s}$, where $v\in S_H$ with $v_\perp\neq 0$. Suppose that the local peak selection p w.r.t. L is continuous at v. Then $t_s\to t$ and $w_{L,s}\to w_L$ as $s\to 0$.*

Based on the previous lemmas, we have the following crucial property under a weak assumption that p is continuous, which improves the results of Lemma 2.1 in [15] and Lemma 2.13 in [27] by changing the domain of the peak selection $p(v)$ from $S_{L^\perp}$ to S_H and relaxing the restriction on v.

LEMMA 3.6. *Let $J\in C^1$ and p be a local peak selection of J w.r.t. L at $v\in S_H$ with $v_\perp\neq 0$, $d=-\nabla J(p(v))\neq 0$. If p is continuous at v, then*

$$J(p(v(s)))-J(p(v))\leq -ts\|d\|^2+o(s). \tag{3.10}$$

Proof. Denote $\theta=\frac{t_s}{\sqrt{1+s^2\|d\|^2}}v+w_{L,s}$. The continuity of p at v, Lemma 3.3 and Lemma 3.5 state that

$$p(v(s))\to p(v) \quad \text{and} \quad \theta\to p(v) \quad \text{as} \quad s\to 0^+.$$

By definition, $p(v)$ is a local maximizer of J on the half subspace $[L,v]$. Thus, for $s>0$ small enough, the mean value theorem yields

$$J(p(v(s)))-J(p(v))\leq J(p(v(s)))-J(\theta)=\frac{t_s s}{\sqrt{1+s^2\|d\|^2}}\langle J'(\xi),d\rangle, \tag{3.11}$$

with $\xi=\xi(s)=\mu p(v(s))+(1-\mu)\theta$ for some $\mu=\mu(s)\in(0,1)$, where $\theta\in[L,v]$ is used. The facts that $p(v(s))\to p(v)$, $\theta\to p(v)$ as $s\to 0^+$, and $\mu=\mu(s)\in(0,1)$, combined with the triangle inequality imply that, when $s\to 0^+$,

$$\|\xi-p(v)\|=\|\mu p(v(s))+(1-\mu)\theta-p(v)\|\leq \mu\|p(v(s))-p(v)\|+(1-\mu)\|\theta-p(v)\|\to 0.$$

Thus, due to $J\in C^1$, we have

$$\|J'(\xi)-J'(p(v))\|\to 0 \quad \text{as } s\to 0^+. \tag{3.12}$$

Then, by employing the Cauchy-Schwartz inequality and Lemma 3.5, for $s>0$ small enough, (3.11) and (3.12) lead to

$$\begin{aligned}
J(p(v(s)))-J(p(v)) &\leq \frac{t_s s}{\sqrt{1+s^2\|d\|^2}}\Big(\langle J'(p(v)),d\rangle+\langle J'(\xi)-J'(p(v)),d\rangle\Big)\\
&\leq \frac{t_s s}{\sqrt{1+s^2\|d\|^2}}\Big(-\|d\|^2+\|J'(\xi)-J'(p(v))\|\|d\|\Big)\\
&=-t_s\frac{s\|d\|^2}{\sqrt{1+s^2\|d\|^2}}+o(s)\\
&=-ts\|d\|^2+\left(t-\frac{t_s}{\sqrt{1+s^2\|d\|^2}}\right)s\|d\|^2+o(s)\\
&=-ts\|d\|^2+o(s).
\end{aligned} \tag{3.13}$$

The proof is completed. □

Then the following lemma is a straightforward result of Lemma 3.6.

LEMMA 3.7. *Let $v\in S_H$ with $v_\perp\neq 0$. If $J\in C^1$ has a local peak selection p w.r.t. L at v, i.e., $p(v)=tv+w_L$, s.t. (i) p is continuous at v; (ii) $t>0$; (iii) $\|d\|>0$, then for any $\sigma\in(0,1)$, there is $\delta>0$, s.t.,*

$$J(p(v(s)))-J(p(v))<-\sigma ts\|d\|^2, \quad \forall 0<s<\delta. \tag{3.14}$$

Now we proceed to show the feasibility of the normalized Goldstein search rule stated in Definition 3.1 for its implementation in the NG-LMA, which will be introduced in Section 4. It will be noted that, once an initial ascent direction $v^0 = v^0_\perp + v^0_L \in S_H$ with $v^0_\perp \in L^\perp$, $v^0_L \in L$, $v^0_\perp \neq 0$, is chosen in the NG-LMA, the closed set $\mathbb{U} \subset S_{[L^\perp, v^0_L]} \subset S_H$ defined by

$$\mathbb{U} = \{v = v_\perp + \tau v^0_L \in S_{[L^\perp, v^0_L]} : v_\perp \in L^\perp, 0 \leq \tau \leq 1\}, \tag{3.15}$$

contains all functions v^k generated by the algorithm. Meanwhile, from (3.1) and (3.2), $v(s) \in \mathbb{U}$ if $v \in \mathbb{U}$. Consequently, in the discussion below, the domain of the peak selection p is limited to $\mathbb{U} \subset S_H$ rather than S_H, unless specified.

THEOREM 3.1. *Suppose $J \in C^1$ and p is a local peak selection of J w.r.t. L at $v \in \mathbb{U}$ with $v_\perp \neq 0$ and $p(v) = tv + w_L$. Further assume that (i) p is continuous at v; (ii) $t > 0$; (iii) $\|d\| > 0$; (iv) $\inf_{v \in \mathbb{U}} J(p(v)) > -\infty$. Then for any given constants σ_1, σ_2 with $0 < \sigma_2 < \sigma_1 < 1$, there exist two constants $\bar{s}_1$, $\bar{s}_2$ with $0 < \bar{s}_1 < \bar{s}_2$, s.t. for any $s \in (\bar{s}_1, \bar{s}_2)$, it satisfies the normalized Goldstein search rule, i.e.,*

$$-\sigma_1 ts\|d\|^2 < J(p(v(s))) - J(p(v)) < -\sigma_2 ts\|d\|^2. \tag{3.16}$$

Proof. Denote

$$\varphi^\sigma_v(s) = J(p(v(s))) - J(p(v)) + \sigma st\|d\|^2, \quad \sigma \in (0,1). \tag{3.17}$$

Obviously it is only needed to prove that there exists a bounded interval $(\bar{s}_1, \bar{s}_2) \subset (0, \infty)$, s.t. $\varphi^{\sigma_1}_v(s) > 0$ and $\varphi^{\sigma_2}_v(s) < 0$ for any $s \in (\bar{s}_1, \bar{s}_2)$. Lemma 3.7 states that for any $\sigma \in (0,1)$, there exists a constant $\delta > 0$, s.t., for any $s \in (0, \delta)$, $\varphi^\sigma_v(s) < 0$. As a result, for σ_i, $i = 1,2$, there exists δ_1, s.t. $\varphi^{\sigma_i}_v(s) < 0$, for any $s \in (0, \delta_1)$. On the other hand, the fact that $v(s) \in \mathbb{U}$ and condition (iv) lead to

$$J(p(v(s))) \geq \inf_{v \in \mathbb{U}} J(p(v)) > -\infty. \tag{3.18}$$

Due to the conditions (ii), (iii) and (3.18), we have

$$\lim_{s \to +\infty} \varphi^\sigma_v(s) = +\infty. \tag{3.19}$$

Since $J \in C^1$, p is continuous at v and $v(s)$ is continuous w.r.t. s, $\varphi^\sigma_v(s)$ is continuous w.r.t. s also. Consequently, the combination of (3.19) and the fact of $\varphi^{\sigma_2}_v(s) < 0$ for $s \in (0, \delta_1)$ implies that $\varphi^{\sigma_2}_v(s) = 0$ has at least one root in $(0, \infty)$. Set

$$\bar{s}_2 = \bar{s}_2(v) := \min\{\bar{s} > 0 : \varphi^{\sigma_2}_v(\bar{s}) = 0\} > \delta_1 > 0. \tag{3.20}$$

It is true that $\varphi^{\sigma_2}_v(s) < 0$ for each $s \in (0, \bar{s}_2)$. Actually we can prove it by contradiction argument. Suppose that there exists $\bar{s}_3 \in (0, \bar{s}_2)$, s.t. $\varphi^{\sigma_2}_v(\bar{s}_3) \geq 0$. Since $\varphi^{\sigma_2}_v(s) < 0$ for any $s \in (0, \delta_1)$, there exists $\bar{s}_4 \in (0, \bar{s}_3] \subset (0, \bar{s}_2)$, s.t. $\varphi^{\sigma_2}_v(\bar{s}_4) = 0$. The fact $\bar{s}_4 < \bar{s}_2$ is a contradiction to the definition of $\bar{s}_2$.

Note that $0 < \sigma_2 < \sigma_1 < 1$, (3.17) leads to $\varphi^{\sigma_1}_v(\bar{s}_2) > \varphi^{\sigma_2}_v(\bar{s}_2) = 0$. Thus $\varphi^{\sigma_1}_v(s) = 0$ also has at least one root in $(0, \bar{s}_2)$. Set

$$\bar{s}_1 = \bar{s}_1(v) := \max\{\bar{s} \in (0, \bar{s}_2) : \varphi^{\sigma_1}_v(\bar{s}) = 0\} > \delta_1 > 0. \tag{3.21}$$

We claim that $\varphi^{\sigma_1}_v(s) > 0$ for each $s \in (\bar{s}_1, \bar{s}_2)$, which can be verified by contradiction argument similarly as above. ∎

Lemma 3.8. *Suppose that the same assumptions of Theorem 3.1 hold. Denote* $\bar{s}_0$ *as the least positive sign-changing point of* $\varphi_v^{\sigma_1}(s)$. *Then, for any* $s>0$ *satisfying the left-hand-side inequality of the normalized Goldstein search rule at* v, *i.e.,*

$$-\sigma_1 ts\|d\|^2 < J(p(v(s))) - J(p(v)), \tag{3.22}$$

with σ_1 *the constant as that in Theorem 3.1, there holds that* $s>\bar{s}_0=\bar{s}_0(v)>0$. *Further,*

$$\bar{s}_0=\bar{s}_0(v)=\inf\{s\big|-\sigma_1 ts\|d\|^2<J(p(v(s)))-J(p(v))<-\sigma_2 ts\|d\|^2\}.$$

Proof. In terms of the definition of $\bar{s}_0=\bar{s}_0(v)$ and similar to the proof of Theorem 3.1, it is also true that $\bar{s}_0>0$ and

$$\varphi_v^{\sigma_1}(s)\le 0, \quad \forall s\in(0,\bar{s}_0).$$

Obviously (3.22) leads to $\varphi_v^{\sigma_1}(s)>0$, which, combined with $\varphi_v^{\sigma_1}(\bar{s}_0)=0$, implies $s>\bar{s}_0=\bar{s}_0(v)>0$. Consequently, $\bar{s}_0$ is a lower bound of the Goldstein step-size. On the other hand, by the definitions of $\bar{s}_i, i=0,1,2$, $\bar{s}_0\le\bar{s}_1<\bar{s}_2$. As $\bar{s}_0$ is the least positive sign-changing point of $\varphi_v^{\sigma_1}(s)$ with $\varphi_v^{\sigma_1}(s)\le 0$ for $s\in(0,\bar{s}_0)$ and there exists a small right neighborhood of $\bar{s}_0$, s.t. $\varphi_v^{\sigma_1}(s)>0$ and $\varphi_v^{\sigma_2}(s)<0$, i.e., s in this right neighborhood of $\bar{s}_0$ satisfies the normalized Goldstein search rule. As a result, we have

$$\bar{s}_0=\bar{s}_0(v)=\inf\{s\big|-\sigma_1 ts\|d\|^2<J(p(v(s)))-J(p(v))<-\sigma_2 ts\|d\|^2\}.$$

□

Owing to Lemma 3.8, it is natural to introduce the following definition.

Definition 3.2 (The least Goldstein search step-size). *For two fixed constants* σ_1 *and* σ_2 *with* $0<\sigma_2<\sigma_1<1$, $\bar{s}_0=\bar{s}_0(v)$ *defined in Lemma 3.8 is called the least Goldstein search step-size w.r.t.* L *at* v.

Remark 3.1. Actually Figure 3.1 provides a geometric interpretation of Theorem 3.1 and Lemma 3.8:

(1) The points on the curve $J(p(v(s)))$ w.r.t. s sandwiched between the dotted straight lines in the figures correspond to all acceptable points of the normalized Goldstein search rule. Obviously all $s\in(\bar{s_1},\bar{s_2})$ satisfy the normalized Goldstein search rule. Thus this validates the feasibility of the normalized Goldstein search rule;

(2) All s satisfying the normalized Goldstein search rule have an infimum $\bar{s}_0=\bar{s}_0(v)>0$, which is the least positive sign-changing point of $\varphi_v^{\sigma_1}(s)$. This property will guarantee that the iterative sequence generated by the NG-LMM will not accumulate at some points before the termination condition is satisfied under a natural condition. This will be verified in details in Lemma 5.3.

4. The normalized Goldstein-type local minimax algorithm (NG-LMA)

Based on the discussion above, we will describe the NG-LMA in this section. By Lemma 3.7 and the contradiction argument, following the lines of the proof of Theorem 2.1 in [15], we obtain the following theorem routinely.

Theorem 4.1. *If* J *has a local peak selection w.r.t.* L *at* $\bar{v}\in S_H$ *with* $\|\bar{v}_\perp\|\ne 0$, *which is denoted as* $p(\bar{v})=\bar{t}\bar{v}+\bar{w}_L$, *satisfying (i)* p *is continuous at* $\bar{v}$; *(ii)* $\bar{t}>0$; *(iii)* $\bar{v}$ *is a local minimum point of* $J(p(v))$ *in* S_H, *then* $\bar{u}=p(\bar{v})\notin L$ *is a critical point of* J.

Theorem 4.1 characterizes a saddle point as a local minimax solution. Actually it states that, under the assumptions (i) and (ii), a minimum point $\bar{u}$ of J on $\mathcal{M}$ is a

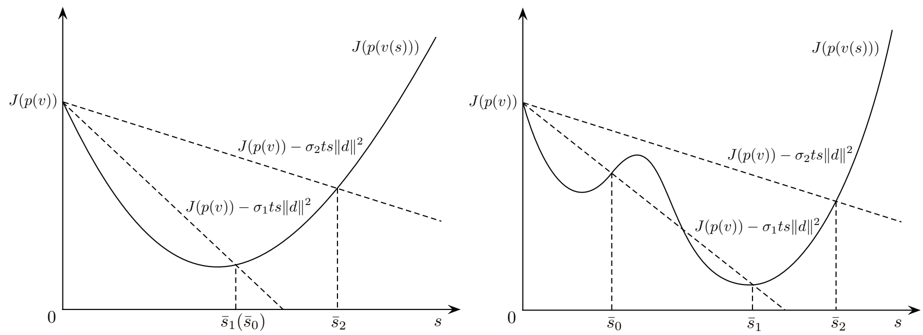

FIG. 3.1. *The illustration for the feasibility of the normalized Goldstein search rule and the existence of the least Goldstein search step-size.*

critical point not in L and so is a new solution different from those in L. As mentioned above, $\bar{u}$ is unstable in H but stable on $\mathcal{M}$ and some descent algorithms can work for the minimization problem in terms of J on $\mathcal{M}$. Consequently, Theorem 4.1 serves as a mathematical justification of the following NG-LMA, which is a stable algorithm for finding unstable solutions.

On the other hand, to establish an existence result for semilinear elliptic PDEs with non-convex generic functional, the following Palais-Smale (P.S.) condition is often used to replace the compactness condition. Actually it will also play a crucial role in the global convergence analysis for our numerical approach in Section 5.

DEFINITION 4.1. *A functional $J\in C^1(H,\mathbb{R})$ is said to satisfy the Palais-Smale (P.S.) condition if any sequence $\{u_n\}_{n=1}^{\infty}\subset H$ satisfying that $J(u_n)$ is bounded and $J'(u_n)\to 0\,(n\to\infty)$, has a convergent subsequence.*

The so-called ascent (descent) direction defined in the following is also needed.

DEFINITION 4.2. *A point $v\in H$ is called an ascent (descent) direction of J at u if there exists $\delta>0$, s.t.,*

$$J(u+tv)>(<)J(u),\quad \forall 0<t<\delta.$$

Now we present the normalized Goldstein-type local minmax algorithm.

Algorithm 4.1. (The NG-LMA).

Step 1. (Initialization) Take an error tolerance $\varepsilon_1>0$, two constants s.t. $0<\sigma_2<\sigma_1<1$ and $n-1$ previously found critical points of J. Set the support $L=\mathrm{span}\{u_1,u_2,\cdots,u_m\}$ where $u_1,u_2,\cdots,u_m$ are m $(m\le n-1)$ previously found critical points and u_m is the one with the highest critical value in $\{u_i\}$ $(1\le i\le m)$. Choose an initial ascent direction $v^0=v_L^0+v_\perp^0\in S_H$ at u_m where $v_L^0\in L$, $0\ne v_\perp^0\in L^\perp$. Set $k=0$, $t^0=1$, $w_L^0=u_m\in L$;

Step 2. (Peak selection) Using $u^k=t^kv^k+w_L^k$ as the initial guess, solve for $p(v^k)$ s.t.

$$J(p(v^k))=\max_{u\in[L,v^k]}J(u),$$

and still denote $u^k=p(v^k)=t^kv^k+w_L^k$;

Step 3. (The steepest descent direction) Compute the steepest descent direction d^k of J at u^k by the definition in (2.3);

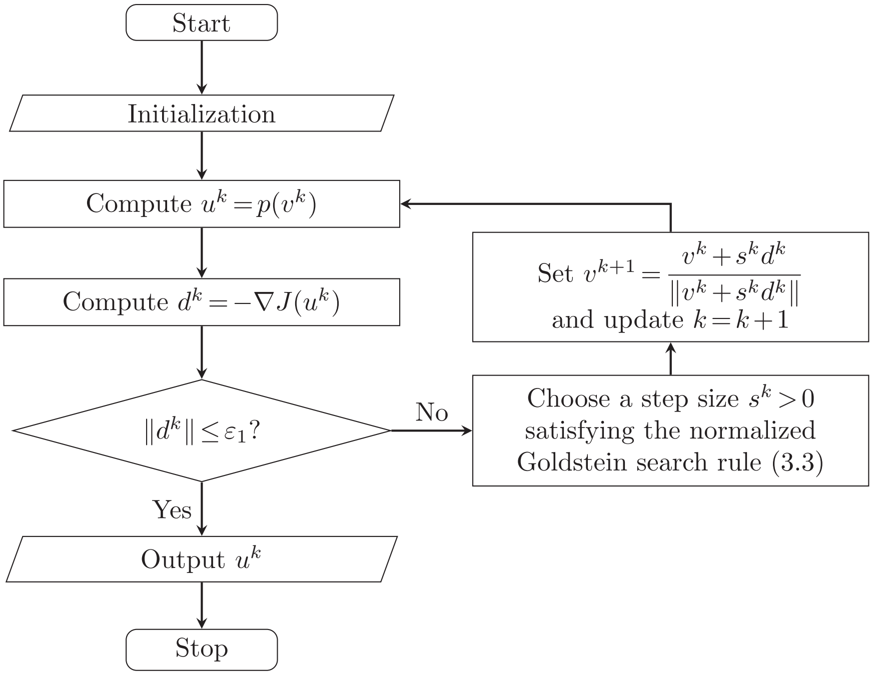

Fig. 4.1. *The flowchart of the NG-LMA.*

Step 4. (Termination) If $\|d^k\| \le \varepsilon_1$, output u^k, and **stop**; else goto **Step 5**;

Step 5. (The normalized Goldstein search) Find

$$v^k(s^k) = \frac{v^k + s^k d^k}{\|v^k + s^k d^k\|},$$

such that s^k satisfies the normalized Goldstein search rule (3.3). As mentioned before, a steepest descent search $v^k(s^k)$ usually leaves the submanifold $\mathcal{M}$ and a return rule is needed for the search to come back to $\mathcal{M}$;

Step 6. (Iteration) Set $v^{k+1} = v^k(s^k)$ and update $k = k+1$, then goto **Step 2**.

In general, it is recommended to set $\sigma_1 = 0.8$ and $\sigma_2 = 0.2$ in the realization of the NG-LMA. Further, to illustrate the NG-LMA more clearly, a flowchart is depicted in Figure 4.1.

On the other hand, it is worthwhile to point out that the step-size s^k in **Step 5** of the k-th iteration which satisfies the normalized Goldstein search rule is searched by the following procedure.

Algorithm 4.2. The Normalized Goldstein Search Algorithm.

Step 5-1. Take an initial point s_0^k in $[0, +\infty)$ (or $[0, s_{\max}]$, e.g., $s_{\max} = 1$) and a fixed constant $\eta > 1$ (e.g., $\eta = 2$). Compute $J(u^k)$. Set $a_0 := 0$, $b_0 := +\infty$ (or $s_{\max}$) and $j := 0$;

Step 5-2. Compute $J\big(p(v^k(s_j^k))\big)$. Actually the local maximum point $p\big(v^k(s_j^k)\big)$ in $[L, v^k(s_j^k)]$ is computed by using the initial guess $u = t^k v^k(s_j^k) + w_L^k$, where t^k and w_L^k

are those in $u^k = p(v^k) = t^k v^k + w_L^k$. This process is similar to that in **Step 2** and the aim of it is to guarantee the continuity of the peak selection p numerically;

Step 5-3. If

$$J\big(p(v^k(s_j^k))\big) - J(u^k) < -\sigma_2 t^k s_j^k \|d^k\|^2,$$

go on; otherwise, set $a_{j+1} := a_j$, $b_{j+1} := s_j^k$, $s_{j+1}^k := \dfrac{a_{j+1}+b_{j+1}}{2}$ and $j := j+1$, goto **Step 5-2**;

Step 5-4. If

$$J\big(p(v^k(s_j^k))\big) - J(u^k) > -\sigma_1 t^k s_j^k \|d^k\|^2,$$

output $s^k := s_j^k$ and **stop**; otherwise, set $a_{j+1} := s_j^k$, $b_{j+1} := b_j$,

$$s_{j+1}^k := \begin{cases} \dfrac{a_{j+1}+b_{j+1}}{2} & \text{if } b_{j+1} < +\infty, \\ \eta s_j^k, & \text{otherwise,} \end{cases}$$

and $j := j+1$, goto **Step 5-2**.

---

5. Convergence analysis of the NG-LMM

In this section, we establish the convergence analysis for the NG-LMA. One of the main issues is to show the weak version of the homeomorphism of the peak selection $p(v)$ when $v \in \mathbb{U}$. In fact, similar to [26], to relax the requirement on the initial ascent directions, we extend the domain of the peak selection $p(v)$ from $S_{L^\perp}$ to S_H in Definition 2.1. As a result, $p(v)$ is, in general, no longer a homeomorphism. In order to compensate for this shortage, Xie et al. provided a weak version of the homeomorphism in Theorem 2.1 in [26] for the normalized Armijo-type local minimax algorithm (NA-LMA), which is a helpful property for the convergence analysis of the modified LMA. Fortunately, by taking a careful look at the proof, it also holds for the NG-LMA. Another crucial issue is to illustrate that the sequence will not accumulate around a non-critical point. For this purpose, we prove a locally uniform lower bound of the step-size determined by the normalized Goldstein search rule by taking full advantage of the left inequality of the normalized Goldstein search rule. Actually this strategy is completely distinguished from the analysis for the NA-LMA in [26].

For the convergence analysis later, we begin with two corresponding lemmas below. The first lemma is aimed to depict some monotonic properties of the sequence $\{v^k\}$ generated by the NG-LMA and will be used in the proof of the subsequent lemma. The second one is exactly the weak version of the homeomorphism of p. As the proof can be accomplished following the same strategies as those in Lemma 2.3 in [26], herein it is skipped for brevity.

LEMMA 5.1. *Let $\{v^k\} \subset S_H$ be a sequence generated by the NG-LMA. Assume $v^0 = v_\perp^0 + v_L^0 \in S_H$ with $v_\perp^0 \in L^\perp, v_L^0 \in L, v_\perp^0 \neq 0$. Then for any $k = 1,2,\cdots$, we have $v^k = v_\perp^k + \tau^k v_L^0 \in S_H$ for some $v_\perp^k \in L^\perp$, $0 < \tau^{k+1} < \tau^k < 1$ and $\|v_\perp^k\| < \|v_\perp^{k+1}\|$. Furthermore $v_L^k = \tau^k v_L^0$ converges.*

Lemma 5.1 states that there are three monotonic properties in the algorithm for all $v^k = v_\perp^k + v_L^k, k = 1,2,\cdots$, namely,

$$J(p(v^{k+1})) < J(p(v^k)), \quad \|v_\perp^{k+1}\| > \|v_\perp^k\|, \quad \|v_L^{k+1}\| < \|v_L^k\|. \tag{5.1}$$

Further, it implies that, once an initial ascent direction $v^0 = v^0_\perp + v^0_L$ is chosen in the NG-LMA with $v^0_\perp \in L^\perp$, $\|v^0_\perp\| \neq 0$, $v^0_L \in L$, all functions v^k generated by the NG-LMA are in the closed subset $\mathbb{U}$ of S_H with

$$\mathbb{U} = \{v = v_\perp + \tau v^0_L \in S_{[L^\perp, v^0_L]} : v_\perp \in L^\perp, 0 \le \tau \le 1\}.$$

That is the reason why the domain of the peak selection p is only limited to be $\mathbb{U} \subset S_H$ instead of S_H in Section 3. On the other hand, to guarantee the sequence $\{v^k\}$ to depart from L, we only need to take v^0, s.t. $\|v^0_L\| < 1$ or $\|v^0_\perp\| > 0$, i.e., v^0 leaves L rather than lies in L.

LEMMA 5.2. *Let $\{v^k\} \subset \mathbb{U}$ be a sequence generated by the NG-LMA taking the initial ascent direction v^0 with $v^0_\perp \neq 0$. Assume (i) p is continuous in $\mathbb{U}$; (ii) $t_k \ge \alpha > 0, \forall k = 0,1,2,\cdots$. Then $p(v^k) = t^k v^k + w^k_L \to p^* \in H$ implies that there exists $v^* \in \mathbb{U}$ such that $v^k \to v^* \notin L$ and $p(v^*) = p^* \notin L$.*

Lemma 5.2 is the weak version of the homeomorphism of p, which is the same as Theorem 2.1 in [26].

The following lemma guarantees that the sequence generated by the NG-LMA will not accumulate at some point before the termination condition is satisfied.

LEMMA 5.3. *Let $J \in C^1$, $p(\bar v) = \bar t \bar v + \bar w \in [L, \bar v]$ with $\bar v_\perp \neq 0$ be a local peak selection of J w.r.t. L at $\bar v$ and $\bar s_0(v)$ be the least Goldstein search step-size at v defined in Definition 3.2. Assume (i) both $p(v)$ and $\bar s_0 = \bar s_0(v)$ are continuous around $\bar v$; (ii) $\bar t > 0$; (iii) $\|\bar d\| = \|d(\bar v)\| > 0$. Denote $s(v)$ a step-size at v determined by the normalized Goldstein search rule* (3.3). *Then there exists a neighborhood V of $\bar v$ and $s_0 > 0$, s.t. $s(v) \ge s_0 > 0$ for every $v \in V \cap \mathbb{U}$.*

Proof. Set $s_0 = \bar s_0(\bar v)/2$ with $\bar s_0(\bar v) > 0$ the least Goldstein search step-size at $\bar v$. By condition (i), $\bar s_0(v)$ is continuous around $\bar v$. Therefore there exists a neighborhood V of $\bar v$, s.t. $\bar s_0(v) > s_0 > 0$ for every $v \in V \cap \mathbb{U}$. According to Lemma 3.8, for the step-size $s(v)$ determined by the normalized Goldstein search rule (3.3), we have $s(v) > \bar s_0(v) > s_0 > 0$ for every $v \in V \cap \mathbb{U}$. Then we draw the conclusion. ◻

At this point, we are ready to prove the global convergence for the NG-LMA as follows, which is the main result of this paper.

THEOREM 5.1. *Let J satisfy the (P.S.) condition, $p(v)$ be a local peak selection of J w.r.t. L at v, $\bar s_0(v)$ be the least Goldstein step-size at v and $\{v^k\}$ and $\{u^k\}$ be the sequences generated by the NG-LMA with $\varepsilon_1 = 0$, s.t. $u^k = p(v^k) = t^k v^k + w^k_L \in [L, v^k]$ and $v^k \in \mathbb{U}$. If (i) both p and $\bar s_0$ are continuous in $\mathbb{U}$; (ii) $t_k \ge \alpha > 0, \forall k = 0,1,2,\cdots$; (iii) $\inf_{v\in\mathbb{U}} J(p(v)) > -\infty$, then there exists a subsequence $\{v^{k_i}\}_{i=1}^\infty$ s.t. $v^{k_i} \to v^* \in S_H \setminus L$ and $u^{k_i} = p(v^{k_i}) \to u^* = p(v^*) \notin L$ with $J'(u^*) = 0$. If, in addition, u^* is isolated, then $v^k \to v^*$ and $u^k \to u^*$.*

Proof. As in the notation of Algorithm 4.1, we have $u^k = p(v^k)$, $d^k = -\nabla J(u^k)$, and s^k is the step-size satisfying the normalized Goldstein search rule at v^k. By the right inequality of the normalized Goldstein search rule, we have

$$J(u^{k+1}) - J(u^k) < -\sigma_2 t^k s^k \|d^k\|^2. \tag{5.2}$$

Since $J(u^k)$ is monotonically decreasing and bounded from below, it should converge. We claim that $\{u^k\}$ is a (P.S.) sequence, which can be verified by contradiction argument. Suppose that there exists a positive constant δ, s.t. $\|d^k\| > \delta > 0$ for $\forall k > K$ with

$K\in\mathbb{N}^+$ appropriately large. In terms of (5.2) and the condition (ii),

$$J(u^{k+1})-J(u^k)<-\sigma_2\alpha\delta s^k\|d^k\|,\quad \forall k>K. \tag{5.3}$$

Adding up (5.3), we get

$$\sum_{k=K+1}^{\infty}\big(J(u^{k+1})-J(u^k)\big)\le-\sigma_2\alpha\delta\sum_{k=K+1}^{\infty}s^k\|d^k\|. \tag{5.4}$$

Condition (iii) and the monotonic decrease of $J(u^k)$ imply $\sum_{k=0}^{\infty}(J(u^k)-J(u^{k+1}))$ is convergent. This fact, combined with (5.4), leads to the convergence of $\sum_{k=0}^{\infty}s^k\|d^k\|$. As a result,

$$s^k\|d^k\|\to 0,\quad s^k\to 0\quad \text{as}\quad k\to\infty, \tag{5.5}$$

where, the second fact is due to the fact $\|d^k\|>\delta>0$ for $\forall\, k>K$.

On the other hand, thanks to the convergence of $\sum_{k=0}^{\infty}s^k\|d^k\|$, by Lemma 3.3,

$$\|v^{k+1}-v^k\|=\|v^k(s^k)-v^k\|<s^k\|d^k\|,\quad \text{for } s^k>0, \tag{5.6}$$

which means that $\{v^k\}$ is a Cauchy sequence. Then $\{v^k\}$ converges to some $\bar{v}\in\mathbb{U}$. Due to the fact $J(u)\in C^1$ and the continuity of p in $\mathbb{U}$ and $\|d^k\|=\|\nabla J(p(v^k))\|>\delta>0$ for $\forall k>K$, we have $\|\nabla J(p(\bar{v}))\|\ge\delta>0$. By Lemma 5.3, there exists a positive constant s_0, s.t. if $v\in\mathbb{U}$ is close to $\bar{v}$ sufficiently, $s(v)>s_0>0$. Especially $s^k=s(v^k)>s_0>0$ for k large enough. It is a contradiction to (5.5). Therefore there exists a subsequence $\{u^{k_i}\}_{i=0}^{\infty}$ s.t. $J'(u^{k_i})\to 0$ as $i\to\infty$ and $J(u^{k_i})$ converges. By the (P.S.) condition, $\{u^{k_i}\}_{i=0}^{\infty}$ possesses a subsequence, still denoted by $\{u^{k_i}\}$ again, that converges to a critical point.

Finally, using the property verified in Lemma 5.2 to replace the homeomorphism condition and follow the lines of the original proof for the global sequence convergence in [33], we draw the conclusion. □

Remark 5.1. Since $\text{dist}(p(v^k),L):=\inf_{w\in L}\|p(v^k)-w\|=\|t^kv_\perp^k\|=t^k\|v_\perp^k\|$ and $0<\|v_\perp^0\|\le\|v_\perp^k\|\le 1$, condition (ii) in Theorem 5.1 is equivalent to the separable condition of $p(v^k)$ and L depicted by $\text{dist}(p(v^k),L)\ge\beta>0$ for some constant $\beta>0$ in [15,16,26]. If L is spanned by some previously found solutions, then this condition will also guarantee that the computed solution must be a new one not included in the support L. In fact, for some special cases in [15, 26], the local peak selection can be given exactly and the assumption $\text{dist}(p(v^k),L)\ge\beta>0$ can be proven strictly for $L=\{0\}$. While for the general cases, the definition of the local peak selection is a little bit abstract and complicated and the assumption $\text{dist}(p(v^k),L)\ge\beta>0$ is hard to be verified rigorously. Fortunately, it is easy to numerically check this assumption in practical computation. Our computational experiences show that in most cases all t_k satisfy this assumption if the initial ascent direction v^0 is chosen far away from L. If it is not satisfied at some iterative step, i.e., $t^k\approx 0$ for some k, the algorithm can still move on, but it may fail to find a new critical point not in L. In this case, one can restart the algorithm with different initial data.

6. Numerical experiments

Consider a semilinear elliptic equation as follows:

$$F(x,u)=\varepsilon\Delta u(x)-\lambda u(x)+f\big(x,u(x)\big)=0,\quad x\in\Omega, \tag{6.1}$$

where Ω is a bounded domain in $\mathbb{R}^m$, the parameters $\varepsilon > 0$, $\lambda \geq 0$ and the function $f(x,\xi)$ satisfies the following standard hypotheses:

$(h1)$ $f(x,\xi)$ is locally Lipschitz continuous on $\bar{\Omega} \times \mathbb{R}$.

$(h2)$ There are positive constants a_1 and a_2, s.t.,

$$|f(x,\xi)| \leq a_1 + a_2|\xi|^s, \tag{6.2}$$

where $0 \leq s < \dfrac{m+2}{m-2}$ for $m > 2$. If $m = 2$,

$$|f(x,\xi)| \leq a_1 \exp\big(\phi(\xi)\big), \tag{6.3}$$

where $\phi(\xi)\xi^{-2} \to 0$ as $|\xi| \to \infty$.

$(h3)$ $f(x,\xi) = o(|\xi|)$ as $\xi \to 0$.

$(h4)$ There are constants $\mu > 2$ and $M \geq 0$, s.t., for $|\xi| \geq M$,

$$0 < \mu g(x,\xi) \leq \xi f(x,\xi), \tag{6.4}$$

where $g(x,\xi) = \int_0^\xi f(x,t)dt$.

$(h5)$ $\dfrac{f(x,\xi)}{|\xi|}$ is increasing w.r.t. ξ.

REMARK 6.1. For two-dimensional problem, $(h2)$ is not a substantial restriction; $(h4)$ implies that $f(x,\xi)$ is superlinear.

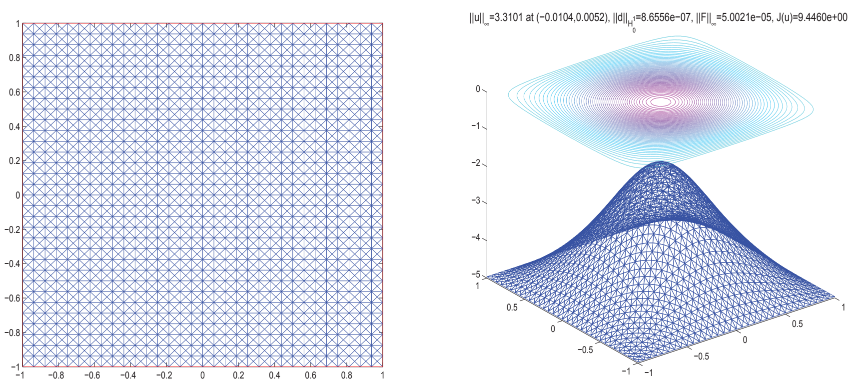

FIG. 6.1. *The coarse mesh grid on a square (left) and the ground state solution u_1 (right) with $L = \{0\}$, $(\tilde{x}_1, \tilde{x}_2) = (-0.5, 0.5)$ and $r = 0.1$ on the square.*

The generic functional associated with the semilinear elliptic Equation (6.1) is

$$J_\varepsilon(u) = \frac{1}{2}\int_\Omega \left(\varepsilon|\nabla u(x)|^2 + \lambda u(x)^2\right)dx - \int_\Omega g\big(x,u(x)\big)dx, \quad u \in H \equiv H_\varepsilon(\Omega), \tag{6.5}$$

where $H \equiv H_\varepsilon(\Omega)$ is a Hilbert space with an ε-dependent inner product and norm defined as

$$\langle u,v\rangle_\varepsilon = \int_\Omega (\varepsilon \nabla u \cdot \nabla v + uv)dx, \quad \|u\|_\varepsilon^2 = \int_\Omega (\varepsilon|\nabla u|^2 + u^2)dx.$$

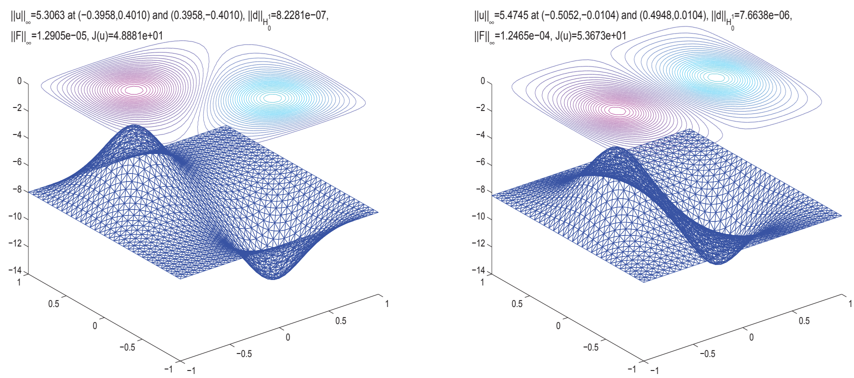

FIG. 6.2. *Two sign-changing solutions* u_2 *(left) with* $L=\text{span}\{u_1\}$, $(\tilde{x}_1,\tilde{x}_2)=(-0.5,0.5)$ *and* $r=0.1$ *and* u_3 *(right) with* $L=\text{span}\{u_1\}$, $(\tilde{x}_1,\tilde{x}_2)=(-0.5,0)$ *and* $r=0.1$ *on the square.*

Actually the ε-dependent norm is equivalent to the standard H^1 norm

$$\|u\|_{H^1}^2=\int_\Omega(|\nabla u|^2+u^2)dx.$$

According to [20], it is easy to prove that, under the hypotheses $(h1)$-$(h4)$, J_ε is C^1 and satisfies the (P.S.) condition, which plays an important role in our theoretical analysis as mentioned before. In addition, J_ε has a mountain pass structure with 0 a local minimum point of J_ε. Further, under hypotheses $(h1)$-$(h5)$, the uniqueness of a local peak selection $p(v)$ of J_ε in $[L,v]$ implies its continuity at v.

It is noted that all $f(x,\xi)$ in the following have the forms of power function $f(x,\xi)=|x|^l\xi^\jmath$ with $l\geq 0$ and $\jmath>2$, which guarantee the assumptions $(h1)$-$(h5)$. In this section we shall first display profiles of multiple solutions to Lane-Emden equation and Henon equation on square and dumbbell domains. Then we shall illustrate multiple solutions to the limiting stationary Gierer-Meinhardt equation. In order to show a solution u_n's profile and contour more clearly, a vertical translation $u_n-1.5\max u_n(x)$ is introduced in the figures below. Unless specified, 32768 triangular elements are used to decompose the domain Ω in our numerical tests. However, in order to see the mesh grids in the figures clearly, a coarse mesh (e.g., see the left of Figure 6.1 with 4096 triangle elements) is employed to redraw the profiles and contours. It is worthwhile to point out that the steepest descent direction d^k can be found by many existing numerical algorithms, e.g., a finite element method, a finite difference method, or a spectral method. In our numerical code, a MATLAB subroutine `assempde`, which is based on the finite element method, is called for getting d^k, while a MATLAB subroutine `fminunc/fminsearch` is implemented to compute the local peak selection at v^k, $u^k=p(v^k)$. Moreover, the stopping criteria $\|d^k\|_H<\varepsilon_1$ (e.g., $\varepsilon_1=5\times10^{-4}$) is utilized to terminate the iteration. Meanwhile we also display the maximum norm of the residual of the model equation, i.e., $\|F\|_\infty$, to monitor the accuracy of our numerical computation. Furthermore, more information on a numerical solution, e.g., its energy and peak locations, can be found by zooming in at the top portion of its figure. Although many numerical results for Ω being a square, dumbbell, L-shaped area or concentric-ring domain, and so on, have been gotten, we only show some typical numerical results on a square or dumbbell domain owing to the limit of the length of this paper.

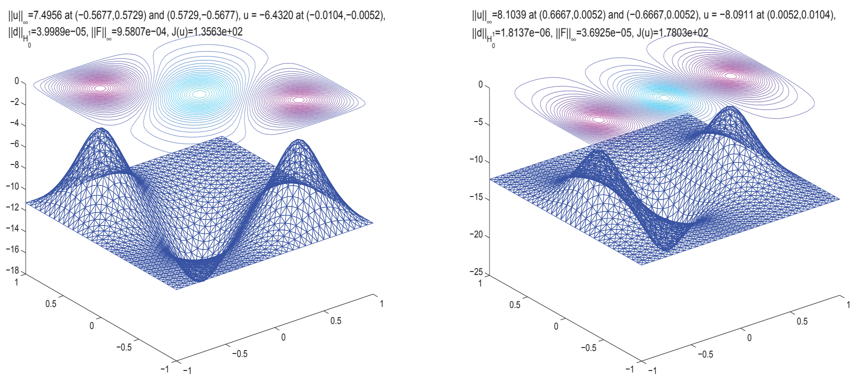

Fig. 6.3. *Two sign-changing solutions* u_4 *(left) with* $L=\text{span}\{u_1,u_2\}$, $(\tilde{x}_1,\tilde{x}_2)=(-0.5,0.5)$ *and* $r=0.1$ *and* u_5 *(right) with* $L=\text{span}\{u_1,u_3\}$, $(\tilde{x}_1,\tilde{x}_2)=(-0.5,0)$ *and* $r=0.1$ *on the square.*

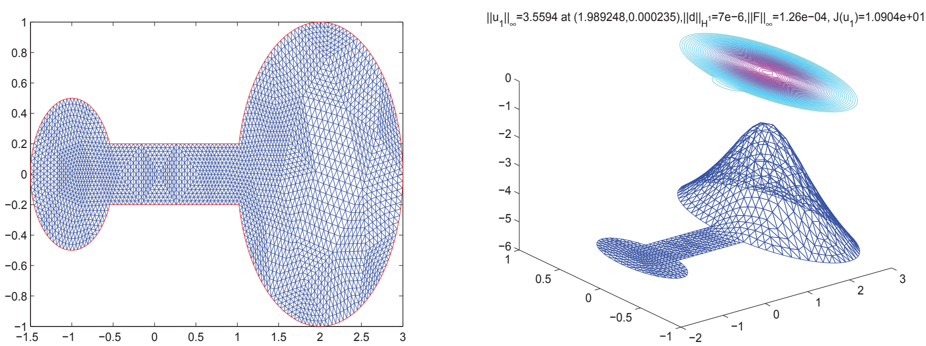

Fig. 6.4. *The coarse mesh grid on a dumbbell (left) and a solution* u_1 *(right) with* $L=\{0\}$, $(\tilde{x}_1,\tilde{x}_2)=(2,0)$ *and* $r=1$ *on the dumbbell.*

Case 1 (Lane-Emden equation): We first present some numerical results for Lane-Emden equation with homogenous Dirichlet boundary condition by setting $\varepsilon=1$, $\lambda=0$ and $f(x,u)=u^{\jmath}(x)$ in (6.1), i.e.,

$$\begin{cases} \Delta u(x)+u^{\jmath}(x)=0, & x\in\Omega, \\ u(x)=0, & x\in\partial\Omega, \end{cases} \tag{6.6}$$

with $\jmath=3$. In this case, we select an initial ascent direction v^0 accordingly by solving

$$\begin{cases} -\Delta v^0(x)=c(x), & x\in\Omega, \\ v^0(x)=0, & x\in\partial\Omega, \end{cases} \qquad c(x)=\begin{cases} 1, \text{ if } |(x_1,x_2)-(\tilde{x}_1,\tilde{x}_2)|\le r, \\ 0, \text{ otherwise}, \end{cases} \tag{6.7}$$

and a normalization followed. Thus the peak-locations $(\tilde{x}_1,\tilde{x}_2)$ of an initial ascent direction can be conveniently selected.

We list profiles and contours of several solutions on a square $\Omega=(-1,1)^2$ in Figures 6.1-6.3 and those of the solutions on a dumbbell Ω in Figures 6.4-6.6. u_1 in the right of Figure 6.1 is the ground state solution, i.e., the least energy solution, which is the unique positive solution of Lane-Emden Equation (6.6) on $\Omega=(-1,1)^2$. Figures 6.2

and 6.3 show two sign-changing solutions with the same Morse index but different symmetries.

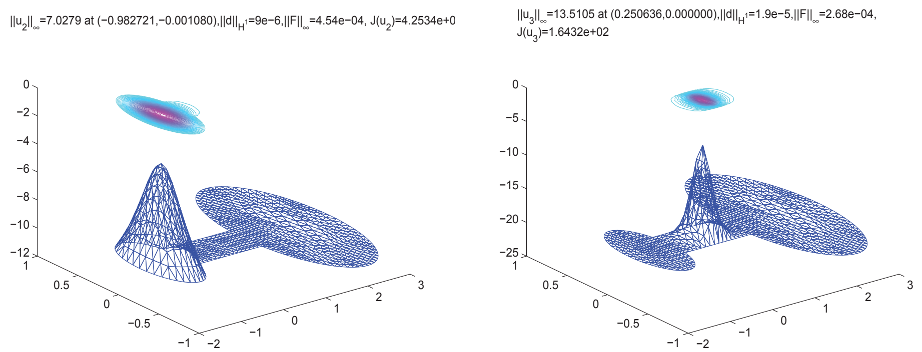

FIG. 6.5. *Two solutions* u_2 *(left) with* $L=\{0\}$, $(\tilde{x}_1,\tilde{x}_2)=(-1,0)$ *and* $r=0.5$ *and* u_3 *(right) with* $L=\{0\}$, $(\tilde{x}_1,\tilde{x}_2)=(0.25,0)$ *and* $r=0.2$ *on the dumbbell.*

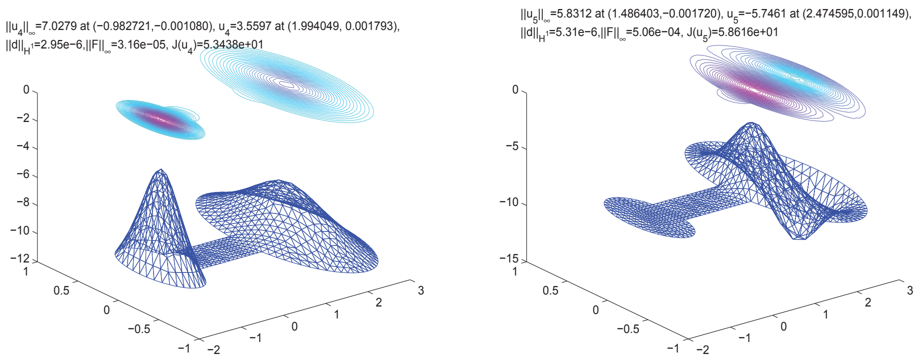

FIG. 6.6. *Two solutions* u_4 *(left) with* $L=\text{span}\{u_1\}$, $(\tilde{x}_1,\tilde{x}_2)=(-1,0)$ *and* $r=0.5$ *and* u_5 *(right) with* $L=\text{span}\{u_1\}$, $(\tilde{x}_1,\tilde{x}_2)=(2,0)$ *and* $r=1$ *on the dumbbell.*

Case 2 (Henon equation): We now present some numerical results for Henon equation with homogenous Dirichlet boundary condition by setting $\varepsilon=1,\lambda=0$ and $f(x,u)=|x|^l u^\jmath(x)$, i.e.,

$$\begin{cases} \Delta u(x)+|x|^\ell u^\jmath(x)=0, & x\in\Omega, \\ u(x)=0, & x\in\partial\Omega, \end{cases} \tag{6.8}$$

with $\ell=6$, $\jmath=3$. Actually Henon equation is a generalization of Lane-Emden equation in astrophysics for the study of rotating stellar structures. The initial ascent direction v^0 is chosen similarly as that in (6.7). Due to the presence of the variable coefficient $|x|^\ell$ in the nonlinear term, the peak of the ground state solution u_1 of Henon equation in Figure 6.7 is closer to the boundary compared with that of Lane-Emden equation, and more and more positive solutions emerge (e.g., u_4, u_5 and u_8 in Figures 6.8-6.10). The profiles and contours of some solutions on the square and dumbbell domain are shown in Figures 6.7-6.10 and Figures 6.11-6.13, respectively.

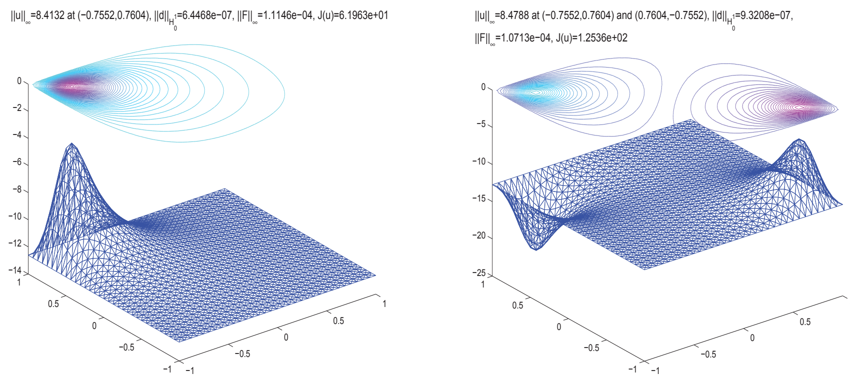

Fig. 6.7. *The ground state solution u_1 (left) with $L=\{0\}$, $(\tilde{x}_1,\tilde{x}_2)=(-0.5,0.5)$ and $r=0.1$ and a solution u_2 (right) with $L=\mathrm{span}\{u_1\}$, $(\tilde{x}_1,\tilde{x}_2)=(0.5,-0.5)$ and $r=0.1$ on the square.*

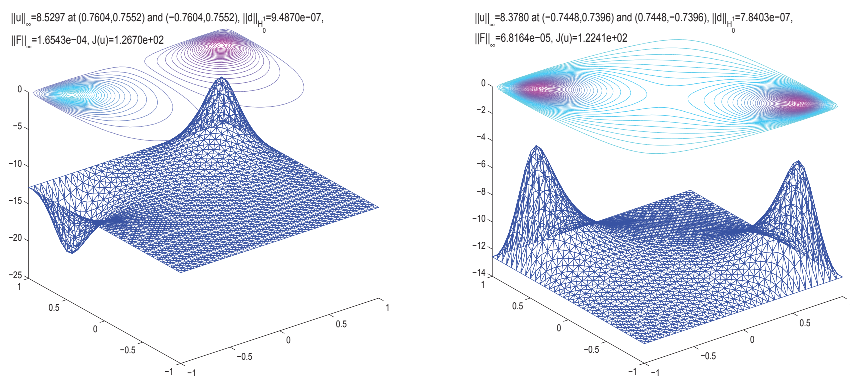

Fig. 6.8. *Two solutions u_3 (left) with $L=\mathrm{span}\{u_1\}$, $(\tilde{x}_1,\tilde{x}_2)=(-0.5,0.5)$ and $r=0.1$ and u_4 (right) with $L=\mathrm{span}\{u_2\}$, $(\tilde{x}_1,\tilde{x}_2)=(-0.5,0.5)$ and $r=0.5$ on the square.*

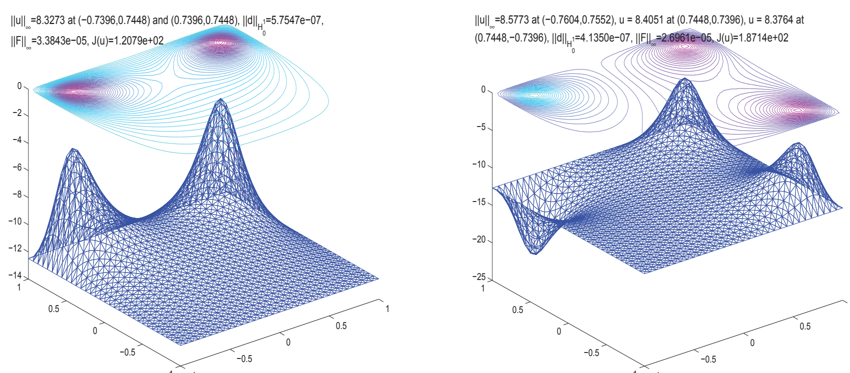

Fig. 6.9. *Two solutions u_5 (left) with $L=\mathrm{span}\{u_3\}$, $(\tilde{x}_1,\tilde{x}_2)=(-0.5,0.5)$ and $r=0.5$ and u_6 (right) with $L=\mathrm{span}\{u_4,u_5\}$, $(\tilde{x}_1,\tilde{x}_2)=(0.5,0.5)$ and $r=0.5$ on the square.*

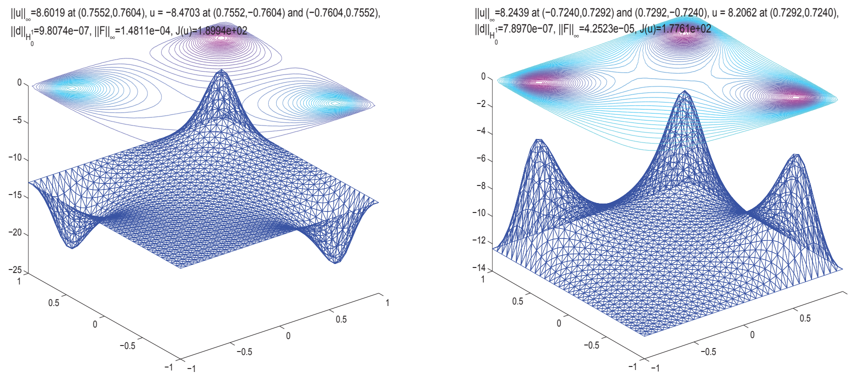

FIG. 6.10. *Two solutions u_7 (left) with $L = \text{span}\{u_1, u_4\}$, $(\tilde{x}_1, \tilde{x}_2) = (0.5, 0.5)$ and $r = 0.5$ and u_8 (right) with $L = \text{span}\{u_6, u_7\}$, $(\tilde{x}_1, \tilde{x}_2) = (0.5, 0.5)$ and $r = 0.5$ on the square.*

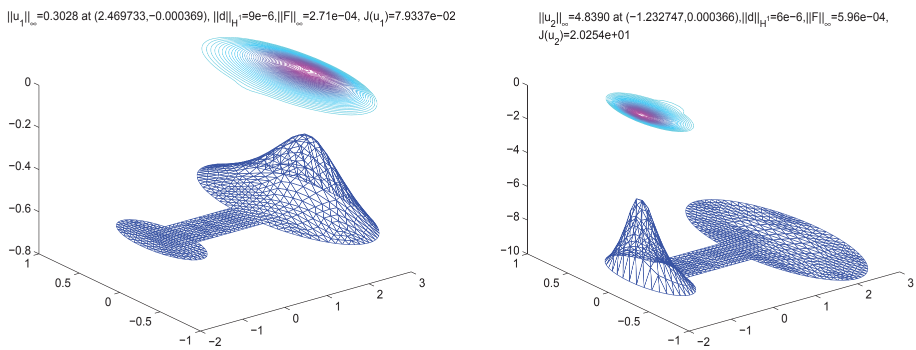

FIG. 6.11. *Two solutions u_1 (left) with $L = \{0\}$, $(\tilde{x}_1, \tilde{x}_2) = (2, 0)$ and $r = 1$ and u_2 (right) with $L = \{u_1\}$, $(\tilde{x}_1, \tilde{x}_2) = (-1, 0)$ and $r = 0.5$ on the dumbbell.*

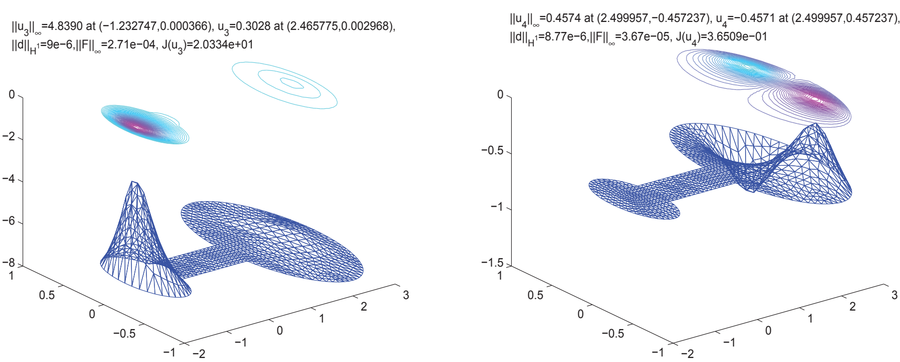

FIG. 6.12. *Two solutions u_3 (left) with $L = \text{span}\{u_2\}$, $(\tilde{x}_1, \tilde{x}_2) = (2, 0)$ and $r = 1$ and u_4 (right) with $L = \text{span}\{u_1\}$, $(\tilde{x}_1, \tilde{x}_2) = (2, 0)$ and $r = 0.5$ on the dumbbell.*

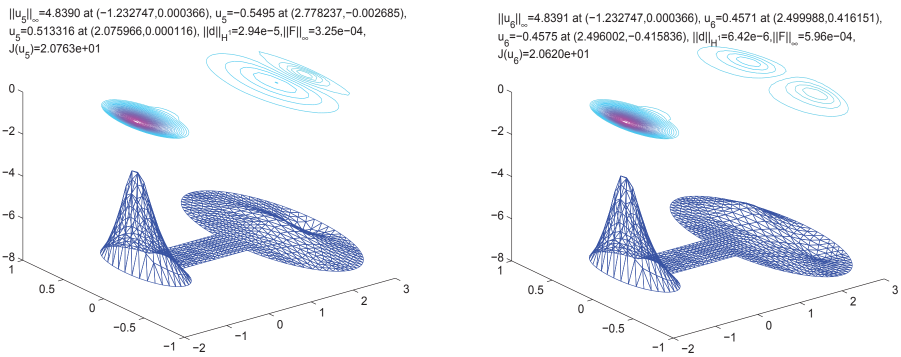

FIG. 6.13. *Two solutions* u_5 *(left) with* $L=\mathrm{span}\{u_1,u_3\}$, $(\tilde{x}_1,\tilde{x}_2)=(0.25,0)$ *and* $r=0.2$ *and* u_6 *(right) with* $L=\mathrm{span}\{u_1,u_4\}$, $(\tilde{x}_1,\tilde{x}_2)=(-1,0)$ *and* $r=0.5$ *on the dumbbell.*

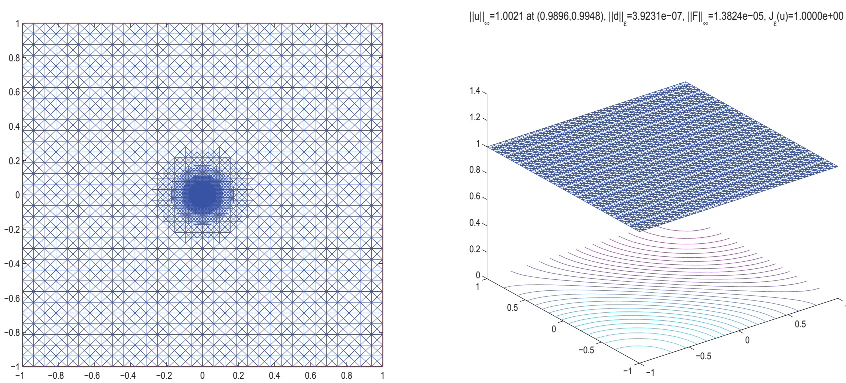

FIG. 6.14. *A coarse four-level locally refined mesh-grid of* Ω *(left) and the trivial solution* $u_\varepsilon^1=1$ *with* $\varepsilon=0.84$ *(right).*

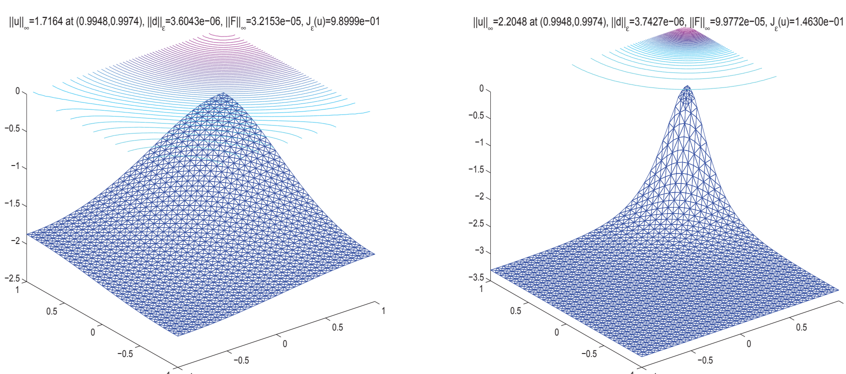

FIG. 6.15. *Two nontrivial least-energy solutions with* $\varepsilon=0.8$ *(left) and* $\varepsilon=0.1$ *(right).*

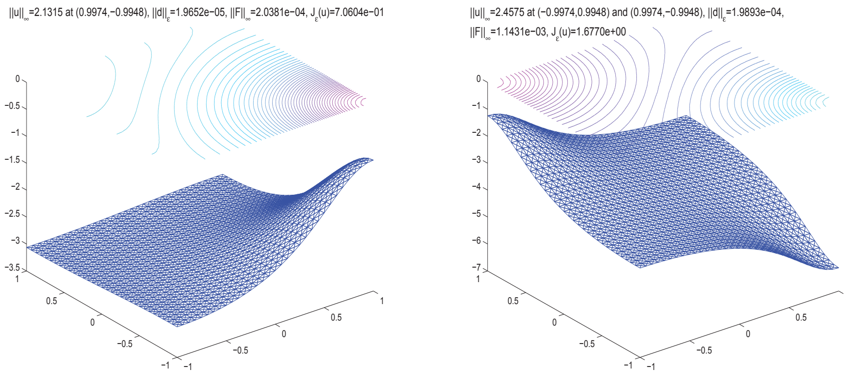

FIG. 6.16. *A positive solution* $u^1_{1/2}$ *with* $v^0(x)=\sin(0.5\pi x_1)$, $L=\{0\}$, $\varepsilon=1/2$ *(left) and a sign-changing solution* $u^2_{1/2}$ *with* $v^0(x)=\sin(0.5\pi x_2)$, $L=\mathrm{span}\{u^1_{1/2}\}$, $\varepsilon=1/2$ *(right).*

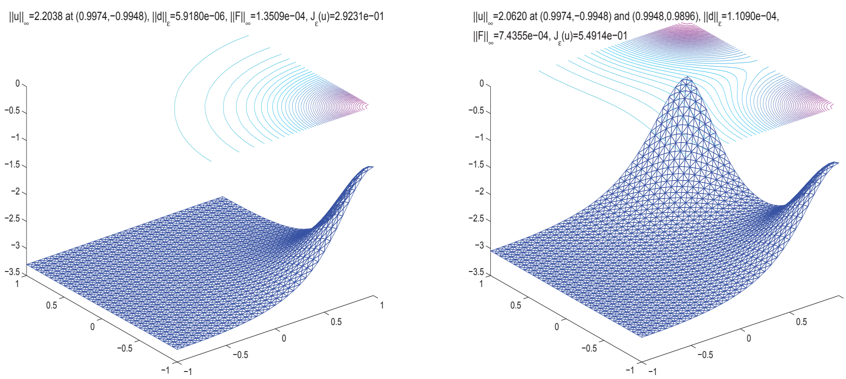

FIG. 6.17. *A positive solution* $u^1_{1/5}$ *with* $v^0(x)=\sin(0.5\pi x_1)$, $L=\{0\}$, $\varepsilon=1/5$ *(left) and a positive solution* $u^2_{1/5}$ *with* $v^0(x)=\sin(0.5\pi x_2)$, $L=\mathrm{span}\{u^1_{1/5}\}$, $\varepsilon=1/5$ *(right).*

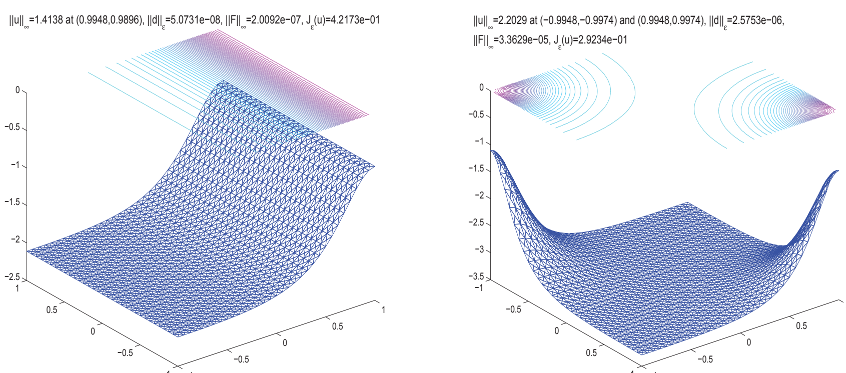

FIG. 6.18. *A positive solution* u_1 *with* $v^0(x)=\sin(0.5\pi x_1)$, $L=\{0\}$, $\varepsilon=0.1$ *(left) and a positive solution* u_2 *with* $v^0(x)=\sin(0.5\pi x_1)\sin(0.5\pi x_2)$, $L=\{0\}$, $\varepsilon=0.1$ *(right).*

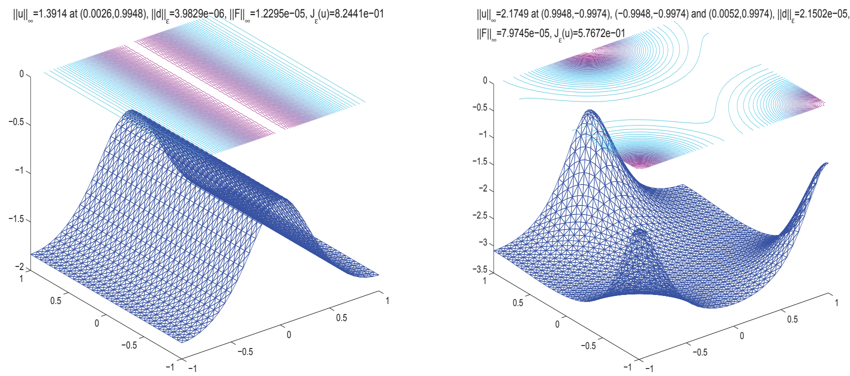

FIG. 6.19. *A positive solution* u_3 *with* $v^0(x) = \cos(\pi x_1)$, $L = \{0\}$, $\varepsilon = 0.1$ *(left) and a positive solution* u_4 *with* $v^0(x) = \cos(\pi x_1)\sin(0.5\pi x_2)$, $L = \{0\}$, $\varepsilon = 0.1$ *(right).*

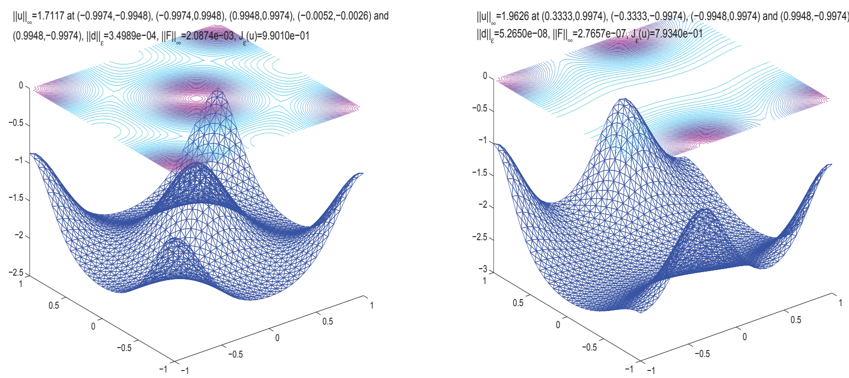

FIG. 6.20. *A positive solution* u_5 *with* $v^0(x) = \cos(\pi x_1)\cos(\pi x_2)$, $L = \{0\}$, $\varepsilon = 0.1$ *(left) and a positive solution* u_6 *with* $v^0(x) = \sin(1.5\pi x_1)\sin(0.5\pi x_2)$, $L = \{0\}$, $\varepsilon = 0.1$ *(right).*

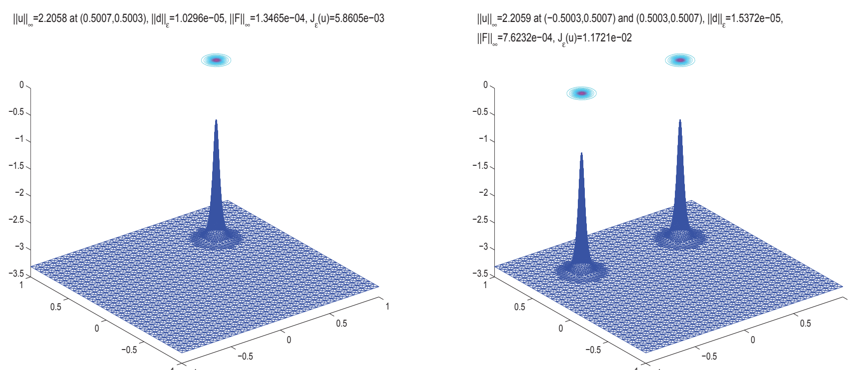

FIG. 6.21. *A interior single-peak solution* u_i^1 *with* $v^0_{(0.5,0.5)}(x)$, $L = \{0\}$, $\varepsilon = 10^{-3}$ *(left) and a interior two-peak solution* u_i^2 *with* $v^0_{(-0.5,0.5)}(x)$, $L = \mathrm{span}\{u_i^1\}$, $\varepsilon = 10^{-3}$ *(right).*

Case 3 (The limiting stationary Gierer-Meinhardt equation): Now we consider the limiting stationary Gierer-Meinhardt equation in biological pattern formation with homogenous Neumann boundary condition on a square by setting $\lambda=1$ and $f(x,u)=|u(x)|^{\jmath-1}u(x)$, i.e.,

$$\begin{cases}\varepsilon\Delta u(x)-u(x)+|u(x)|^{\jmath-1}u(x)=0, & x\in\Omega,\\ \frac{\partial u}{\partial \boldsymbol{n}}=0, & x\in\partial\Omega,\end{cases} \tag{6.9}$$

with ε the singularly perturbed parameter, $\jmath=3$ and $\Omega=(-1,1)^2$.

The initial ascent direction is usually taken as

$$v^0_{x_c}(x)=\begin{cases}\cos^2(0.5\pi|x-x_c|/r), & \text{if} \quad |x-x_c|\le r,\\ 0, & \text{otherwise},\end{cases} \tag{6.10}$$

unless specified, where $x_c\in\bar{\Omega}$ and $r>0$. To guarantee $\|v_0\|=1$ as shown in the NG-LMA in Section 4, a normalization is always followed. For simplicity, we shall not mention it explicitly in the following numerical examples. By appropriately choosing the values of x_c and r, one can guarantee that $v^0_{x_c}(x)$ satisfies the homogeneous Neumann boundary condition and control the position of the peaks of the solutions conveniently. In the following examples, we always set $r=0.5$.

In [26], Xie et al. found and proved the critical perturbation value of ε, i.e.,

$$\varepsilon_c=\frac{\jmath-1}{\lambda_2},$$

where the monotone increasing sequence $\{\lambda_k\}_{k=1}^{\infty}$ are all the eigenvalues of the operator $-\Delta$ in $\Omega=(-1,1)^2$ under the homogenous Neumann boundary condition with $\lambda_1=0$. When $\varepsilon>\varepsilon_c$, the positive solution is only the trivial one $u^1_\varepsilon=1$; when $\varepsilon<\varepsilon_c$, non-trivial positive solutions emerge. In our case, $\varepsilon_c=\frac{\jmath-1}{0.25\pi^2}\approx 0.8106$. Actually, when $\varepsilon>\varepsilon_c$, only the trivial positive solution u^1_ε can be found. Figure 6.14 (right) shows the trivial solution u^1_ε with $\varepsilon=0.84$, which is just a little bigger than ε_c. When $\varepsilon<\varepsilon_c$, the least-energy solutions with unique peak at the corner of $\partial\Omega$ are obtained by taking $v_0=v^0_{(1,1)}(x)$, see Figure 6.15 for $\varepsilon=0.8$ and $\varepsilon=0.1$. We observe that the peak of the least energy solutions becomes sharper and more narrow, with their energy being smaller as the singularly perturbed parameter ε turns to be smaller.

In addition, according to Theorem 3.1 in [26], $\frac{\jmath-1}{\lambda_k}, k=2,3,\cdots$ are bifurcation points for the trivial positive solutions $u^1_\varepsilon=1$. All positive solutions are directly/indirectly generated by these bifurcations from u^1_ε as ε decreases across each bifurcation point $\frac{\jmath-1}{\lambda_k}$. When $\varepsilon_c>\varepsilon>\frac{\jmath-1}{\lambda_3}=\frac{\jmath-1}{0.5\pi^2}\approx 0.4053$, the nontrivial positive solutions can only be the least-energy ones. When $\varepsilon<\frac{\jmath-1}{\lambda_3}$, more and more nontrivial positive solutions emerge.

Figures 6.16-6.17 show solutions when $\frac{\jmath-1}{\lambda_3}<\varepsilon=1/2<\varepsilon_c$ and $0.1621\approx\frac{\jmath-1}{\lambda_5}<\varepsilon=1/5<\frac{\jmath-1}{\lambda_4}\approx 0.2026$, respectively. Each solution on the left of Figures 6.16-6.17 is a positive least-energy solution with MI=1 corresponding to $\varepsilon=1/2$ and $1/5$, respectively. Then put it in the support L and the NG-LMA captures the corresponding sign-changing or positive solutions with MI=2 shown on the right parts. Besides, we have obtained numerous interesting symmetrical or asymmetrical solutions with MI>1 whose existence is still open, e.g., the solutions with the peaks locating along a line and so on. We show some of them in Figures 6.18-6.20 with $0.090\approx\frac{\jmath-1}{\lambda_7}<\varepsilon=0.1<\frac{\jmath-1}{\lambda_6}\approx 0.1013$.

Further, when ε is small enough, due to the existence of interior or boundary layers, the efficiency of the computation depends strongly on the quality of the mesh.

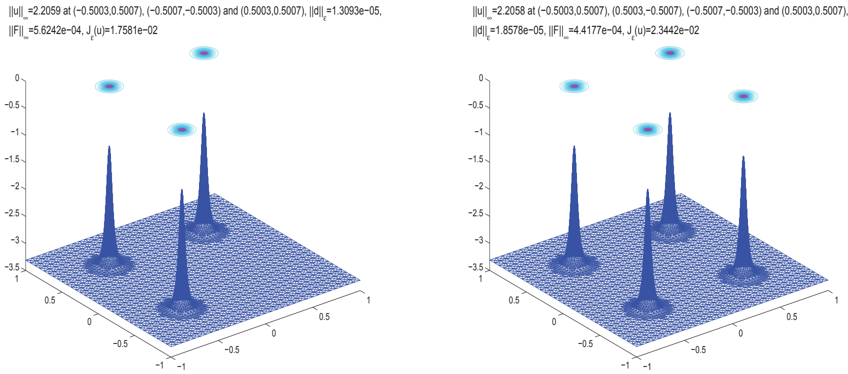

FIG. 6.22. *Two interior multiple-peak solutions* u_i^3 *with* $v^0_{(-0.5,-0.5)}(x)$, $L=\mathrm{span}\{u_i^1,u_i^2\}$, $\varepsilon=10^{-3}$ *(left) and* u_i^4 *with* $v^0_{(0.5,-0.5)}(x)$, $L=\mathrm{span}\{u_i^1,u_i^2,u_i^3\}$, $\varepsilon=10^{-3}$ *(right).*

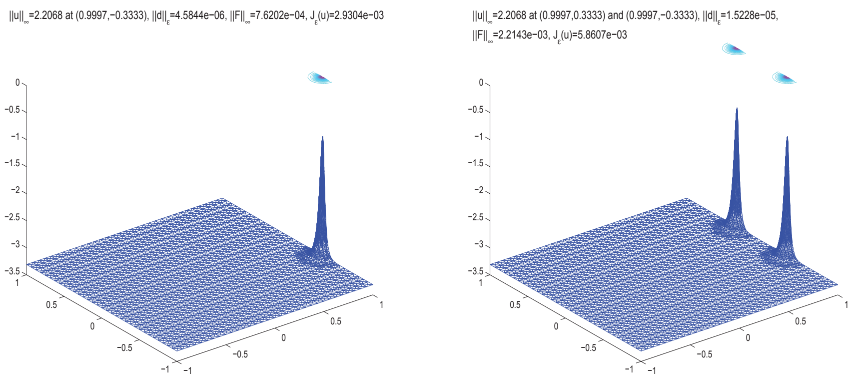

FIG. 6.23. *A boundary-noncorner single-peak solution* u_b^1 *with* $v^0_{(1,-1/3)}(x)$, $L=\{0\}$, $\varepsilon=10^{-3}$ *(left) and a boundary-noncorner two-peak solution* u_b^2 *with* $v^0_{(1,1/3)}(x)$, $L=\mathrm{span}\{u_b^1\}$, $\varepsilon=10^{-3}$ *(right).*

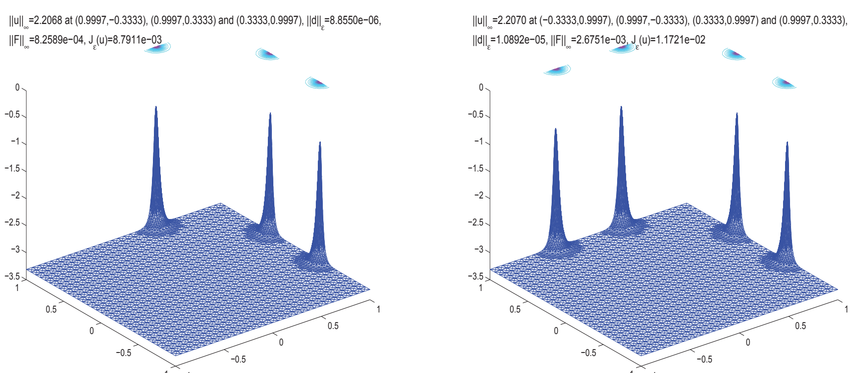

FIG. 6.24. *Two boundary-noncorner multiple-peak solutions* u_b^3 *with* $v^0_{(1/3,1)}(x)$, $L=\mathrm{span}\{u_b^1,u_b^2\}$, $\varepsilon=10^{-3}$ *(left) and* u_b^4 *with* $v^0_{(-1/3,1)}(x)$, $L=\mathrm{span}\{u_b^1,u_b^2,u_b^3\}$, $\varepsilon=10^{-3}$ *(right).*

In this case, we combine a symmetrical mesh with 32768 triangular elements and a local refinement strategy to produce a computational mesh as shown in Figure 6.14

(left). We obtained fruitful interior single-peak solutions, interior multiple-peak solutions, boundary-corner single-peak solutions, boundary-noncorner single-peak solutions (whose peak locates at the boundary point with the minimum mean curvature) and boundary-corner or boundary-noncorner multiple-peak solutions. These solutions are in accordance with the theoretical prediction of [2,12] and the numerical results in [26]. Limited by the length of this paper, we only show some of them in Figures 6.21-6.24. It is noted that the energy of the interior single-peak solutions is always bigger than that of the least-energy solution for the same ε.

7. Concluding remarks

In this paper, a normalized Goldstein-type local minmax algorithm (NG-LMA) is proposed to find multiple minimax-type solutions of semilinear elliptic PDEs. Compared with the normalized Armijo search rule, which needs to control the step-size by using a backtracking strategy, as shown in the classical local minmax method [15,16,26], the normalized Goldstein search rule is composed of two conditions, which not only enable the energy functional to decrease sufficiently, but also prevent the step-size from being too small automatically. The feasibility of the NG-LMA is proven strictly. Further, its global convergence is verified rigorously. Finally, the numerical results of several typical semilinear elliptic equations on square or dumbbell domains are shown to validate the feasibility of our approach. Further, it is worth to mention that the hypothesis of the local Lipschitz-continuity of the peak selection in [26] is replaced by the continuity in $\mathbb{U}$, a subset of S_H, in the theoretical analysis for both the NA-LMA and NG-LMA. Consequently, our work strengthens the mathematical foundation for the LMM.

Acknowledgment. This work was supported by NSFC (91430107, 11771138, 11171104) and the Construct Program of the Key Discipline in Hunan. Yi's work was also partially supported by the Fundamental Research Funds for the Central Universities 531118010207 and the NSFC Grant 11901185.

REFERENCES

[1] L. Armijo, *Minimization of functions having Lipschitz continuous first partial derivatives*, Pac. J. Math., 16(1):1–3, 1966.

[2] D.M. Cao and T. Küpper, *On the existence of multipeaked solutions to a semilinear Neumann problem*, Duke Math. J., 97:261–300, 1999.

[3] G. Chen, J. Zhou, and W.-M. Ni, *Algorithms and visualization for solutions of nonlinear elliptic equations*, Int. J. Bifur. Chaos Appl. Sci. Engrg., 10(07):1565–1612, 2000.

[4] M. Chipot and P. Quittner, *Handbook of Differential Equations: Stationary Partial Differential Equations*, Elsevier/North Holland, 2004.

[5] Y.S. Choi and P.J. McKenna, *A mountain pass method for the numerical solution of semilinear elliptic problems*, Nonlinear Anal., 20(4):417–437, 1993.

[6] G.M. Crippen and H.A. Scheraga, *Minimization of polypeptide energy: XI. The method of gentlest ascent*, Arch. Biochem. Biophys., 144(2):462–466, 1971.

[7] Z. Ding, D. Costa, and G. Chen, *A high-linking algorithm for sign-changing solutions of semilinear elliptic equations*, Nonlinear Anal., 38(2):151–172, 1999.

[8] W. E, W. Ren, and E. Vanden-Eijnden, *String method for the study of rare events*, Phys. Rev. B, 66(5):052301, 2002.

[9] W. E, W. Ren, and E. Vanden-Eijnden, *Simplified and improved string method for computing the minimum energy paths in barrier-crossing events*, J. Chem. Phys., 126(16):164103, 2007.

[10] W. E and X. Zhou, *The gentlest ascent dynamics*, Nonlinearity, 24(6):1831–1842, 2011.

[11] A.A. Goldstein, *On steepest descent*, SIAM J. Control Optim., 3(1):147–151, 1965.

[12] C. Gui, J. Wei, and M. Winter, *Multiple boundary peak solutions for some singularly perturbed Neumann problems*, Ann. Inst. H. Poincaré Anal. Non Linéaire, 17:47–82, 2000.

[13] G. Henkelman and H. Jónsson, *A dimer method for finding saddle points on high dimensional potential surfaces using only first derivatives*, J. Chem. Phys., 111(15):7010–7022, 1999.

[14] D. Li, X. Tong, and Z. Wan, *Numerical Optimization Algorithms and Theory*, Science Press, Beijing, 2010.

[15] Y. Li and J. Zhou, *A minimax method for finding multiple critical points and its applications to semilinear PDEs*, SIAM J. Sci. Comput., 23(3):840–865, 2001.

[16] Y. Li and J. Zhou, *Convergence results of a local minimax method for finding multiple critical points*, SIAM J. Sci. Comput., 24(3):865–885, 2002.

[17] Z. Nehari, *On a class of nonlinear second-order differential equations*, Trans. Amer. Math. Soc., 95(1):101–123, 1960.

[18] W.-M. Ni, *Recent progress in semilinear elliptic equations*, RIMS Kokyuroku, Kyoto University, Kyoto, Japan, 679:1–39, 1989.

[19] M. Powell, *Some global convergence properties of a variable metric algorithm for minimization without exact line searches*, in R.W. Cottle and C. E. Lemke (eds.), Nonlinear Programming, Proc. Sympos. Appl. Math., 9:53–72, 1976.

[20] P.H. Rabinowitz, *Minimax Methods in Critical Point Theory with Applications to Differential Equations*, AMS Bookstore, 65, 1986.

[21] H.B. Schlegel, *Exploring potential energy surfaces for chemical reactions: an overview of some practical methods*, J. Comput. Chem., 24(12):1514–1527, 2003.

[22] W. Sun, C. Xu, and D. Zhu, *Optimization Method*, Science Press, Beijing, 2004.

[23] W. Sun and Y.-X. Yuan, *Optimization Theory and Methods: Nonlinear Programming*, Springer, 98, 2006.

[24] P. Wolfe, *Convergence conditions for ascent methods*, SIAM Rev., 11(2):226–235, 1969.

[25] P. Wolfe, *Convergence conditions for ascent methods. II: Some corrections*, SIAM Rev., 13(2):185–188, 1971.

[26] Z. Xie, Y. Yuan, and J. Zhou, *On finding multiple solutions to a singularly perturbed Neumann problem*, SIAM J. Sci. Comput., 34(1):A395–A420, 2012.

[27] X. Yao, *A minimax method for finding saddle critical points of upper semi-differentiable locally Lipschitz continuous functional in Hilbert space and its convergence*, Math. Comp., 82(284):2087–2136, 2013.

[28] X. Yao and J. Zhou, *A minimax method for finding multiple critical points in Banach spaces and its application to quasi-linear elliptic PDE*, SIAM J. Sci. Comput., 26(5):1796–1809, 2005.

[29] J. Zhang and Q. Du, *Shrinking dimer dynamics and its applications to saddle point search*, SIAM J. Numer. Anal., 50(4):1899–1921, 2012.

[30] L. Zhang, L. Q. Chen, and Q. Du, *Morphology of critical nuclei in solid-state phase transformations*, Phys. Rev. Lett., 98(26):265703, 2007.

[31] L. Zhang, W. Ren, A. Samanta, and Q. Du, *Recent developments in computational modelling of nucleation in phase transformations*, npj Comput. Mater., 2:16003, 2016.

[32] J. Zhou, *Instability analysis of saddle points by a local minimax method*, Math. Comp., 74(251):1391–1411, 2005.

[33] J. Zhou, *Solving multiple solution problems: computational methods and theory revisited*, Commun. Appl. Math. Comput., 31(1):1–31, 2017.